REPORT TITLE:

A HIGH TEMPERATURE ELECTROCHEMICAL ENERGY STORAGE SYSTEM BASED ON SODIUM BETA"-ALUMINA SOLID ELECTROLYTE (BASE)

Type of Report: Final Scientific/Technical Report
Reporting Period Start Date: September 1, 2005
Reporting Period End Date: March 31, 2008
Principal Author: Professor Anil V. Virkar
Date Report Was Issued: June 4, 2008
DOE Award Number: DE-FC26-05NT42623
Name and Address of Submitting Organization:
Department of Materials Science & Engineering
122 S. Central Campus Drive
University of Utah
Salt Lake City, UT 84112

Total Budget: $499,998.00
DOE Portion: $399,998.00
Cost Match: $100,000.00

DISCLAIMER:

ABSTRACT

This report summarizes the work done during the period September 1, 2005 and March 31, 2008. Work was conducted in the following areas: (1) Fabrication of sodium beta" alumina solid electrolyte (BASE) using a vapor phase process. (2) Mechanistic studies on the conversion of α-alumina + zirconia into beta"-alumina + zirconia by the vapor phase process. (3) Characterization of BASE by X-ray diffraction, SEM, and conductivity measurements. (4) Design, construction and electrochemical testing of a symmetric cell containing BASE as the electrolyte and NaCl + $ZnCl_2$ as the electrodes. (5) Design, construction, and electrochemical evaluation of Na/BASE/$ZnCl_2$ electrochemical cells. (6) Stability studies in $ZnCl_2$, $SnCl_2$, and SnI_4, (7) Design, assembly and testing of planar stacks. (8) Investigation of the effect of porous surface layers on BASE on cell resistance.

The conventional process for the fabrication of sodium ion conducting beta"-alumina involves calcination of α-alumina + Na_2CO_3 + $LiNO_3$ at 1250°C, followed by sintering powder compacts in sealed containers (platinum or MgO) at ~1600°C. The novel vapor phase process involves first sintering a mixture of α-alumina + yttria-stabilized zirconia (YSZ) into a dense ceramic followed by exposure to soda vapor at ~1450°C to convert α-alumina into beta"-alumina. The vapor phase process leads to a high strength BASE, which is also resistant to moisture attack, unlike BASE made by the conventional process. The PI is the lead inventor of the process. Discs and tubes of BASE were fabricated in the present work.

In the conventional process, sintering of BASE is accomplished by a transient liquid phase mechanism wherein the liquid phase contains $NaAlO_2$. Some $NaAlO_2$ continues to remain at grain boundaries; and is the root cause of its water sensitivity. In the vapor phase process, $NaAlO_2$ is never formed. Conversion occurs by a coupled transport of Na^+ through BASE formed and of O^{2-} through YSZ to the reaction front. Transport to the reaction front is described in terms of a chemical diffusion coefficient of Na_2O. The conversion kinetics as a function of microstructure is under investigation. The mechanism of conversion is described in this report.

A number of discs and tubes of BASE have been fabricated by the vapor phase process. The material was investigated by X-ray diffraction (XRD), optical microscopy and scanning electron microscopy (SEM), before and after conversion. Conductivity (which is almost exclusively due to sodium ion transport at the temperatures of interest) was measured. Conductivity was measured using sodium-sodium tests as well as by impedance spectroscopy.

Various types of both planar and tubular electrochemical cells were assembled and tested. In some cases the objective was to determine if there was any interaction between the salt and BASE. The interaction of interest was mainly ion exchange (possible replacement of sodium ion by the salt cation). It was noted that Zn^{2+} did not replace Na^+ over the conditions of interest. For this reason much of the work was conducted with $ZnCl_2$ as the cathode salt. In the case of Sn-based, Sn^{2+} did ion

exchange, but Sn^{4+} did not. This suggests that Sn^{4+} salts are viable candidates. These results and implications are discussed in the report.

Cells made with Na as the anode and $ZnCl_2$ as the cathode were successfully charged/discharged numerous times. The key advantages of the batteries under investigation here over the Na-S batteries are: (1) Steel wool can be used in the cathode compartment unlike Na-S batteries which require expensive graphite. (2) Planar cells can be constructed in addition to tubular, allowing for greater design flexibility and integration with other devices such as planar SOFC. (3) Comparable or higher open circuit voltage (OCV) than the Na-S battery. (4) Wider operating temperature range and higher temperature operation than the Na-S battery. (5) If a cell fails, it fails in the short circuit mode unlike Na-S batteries. Also, cells were successfully subjected to several freeze-thaw cycles. Finally, the feasibility of assembling a planar stack was explored. A two cell stack was assembled and tested. A five cell stack was assembled.

TABLE OF CONTENTS

RELEVANCE

The demand for electricity varies depending upon the time of day; low demand during night and high demand during day. In the absence of a commercial energy storage system, virtually all power plants need to be designed for peak power. Thus, there is excess capacity during off-peak periods, which is underutilized. This was one of the principal reasons for the emergence of electrochemical energy storage devices such as batteries, so that power plants can be designed for average demand with the excess energy during off peak periods stored for use later during high peak demands thereby augmenting the capacity of power plants (See Figure 1). This strategy is expected to significantly lower the capital cost. Even with the solid oxide fuel cell (SOFC) technology currently under development for distributed power applications, there are possible options for a similar strategy. For example, if an SOFC can be operated in a reverse mode during off periods, excess capacity available from the grid during the low demand periods can be utilized to electrolyze water and form hydrogen gas for use in many devices, including PEM fuel cells. Thus, during the day SOFC will produce electricity, and during the night it can be used to produce hydrogen – that is, in effect energy is stored in the form of hydrogen during off peak periods. A point to note, however, is that in this scenario, there is the issue of hydrogen storage and conversion to electricity. The potential utility of this approach lies in the use of hydrogen for mobile applications. The roundtrip efficiency of this approach, however, is lower due to the losses associated with re conversion to useful electricity using hydrogen.

During the past three decades, one of the approaches explored has been the use of secondary batteries. One such technology, which is probably one of the most, if not the most, advanced energy storage systems, is based on a solid electrolyte, much in the same as SOFC. The solid electrolyte of interest is Na-β”-alumina solid electrolyte (BASE). The high temperature sodium sulfur battery, invented at Ford Motor Company during the nineteen sixties, has attractive features for such applications. The important features include low materials cost, good durability, high depth of discharge, and potentially low cost. While R & D on many of the storage battery concepts, such as sodium-sulfur, has not been actively pursued in the United States for the past decade or so, a major effort is underway around the world, with commercialization of load leveling batteries well on its way in Japan. Batteries as large as 64 MWh have been successfully deployed in Japan. This project is on the research and development of secondary storage batteries using BASE as the electrolyte, and certain molten salts as the cathode instead of sulfur. The subject batteries can be used for load-leveling, as well as for energy storage, and can be integrated with a power generation system such as an SOFC.

In the case of NGK’s sodium sulfur (NAS) battery, roundtrip efficiency in excess of 90%, lifetime in excess of several years has been demonstrated. The projected cost of the NAS battery for installed capacity of > 400 MWh/year is about $140/kWh, and is expected to go down further with mass penetration into the market place. Thus by all indications, the NAS battery is near commercialization. American Electric Power (AEP) has a couple of NAS batteries installed in the United States under the auspices of DOE.

Despite considerable technical and projected commercial successes, there is considerable room for improvement in the technologies utilizing BASE. The NAS battery does have some shortcomings, all primarily related to the sulfur cathode. The shortcomings are: (a) High cost graphite is needed in the cathode to impart sufficient electronic conductivity to an otherwise insulating sulfur. (b) Sulfur is highly corrosive and attacks the container. Thus, low cost containers cannot be used without protective coatings. A breach in the coating can lead to substantial corrosion. (c) Since sulfur is corrosive, it is not possible to fabricate planar cells, and the design is restricted to tubular cells. This makes the battery less compact than can in principle be achieved with a planar design. (d) If a cell fails, it does so in a high resistance (open circuit) mode. Thus, if one cell in battery pack fails, it renders the entire series leg becomes ineffective.

Work is currently underway on the development of batteries based on either $NiCl_2$ or $FeCl_2$ as the cathode. These batteries are known as ZEBRA batteries. They exhibit relatively high open circuit voltage. However, they too are corrosive, and preclude the use of a planar design. In fact, the so-called inverted design is under development in which the salt cathode is placed inside the BASE tube. This lowers the overall specific energy of the battery.

The battery concept being pursued in this project has the potential to overcome these shortcomings of the NAS as well as the ZEBRA batteries. One of the cathodes being explored is $ZnCl_2$, which yields about the same OCV (or slightly higher) as the NAS battery (about 2 V), can be operated over a wide temperature range, and one can use steel wool for the cathode and also steel for the container. This also makes it possible to design planar batteries. Also, when a cell fails, it does so in low resistance mode. Thus, even if a cell fails, the series leg remains functional.

EXECUTIVE SUMMARY

This project is on research and development of a novel electrochemical energy storage system using sodium-β"-alumina solid electrolyte (BASE), which is a sodium ion conductor with a very high ionic conductivity at 300^{o}C, compared to known oxygen ion conductors. Additionally, the thermodynamic stability of BASE against reduction or development of electronic conduction is far greater than that of oxygen ion conductors such as yttria-stabilized zirconia (YSZ). This presents an excellent opportunity to explore electrochemical energy conversion or storage devices using BASE.

Motivation for the proposed work is the recent emergence of sodium (Na) - sulfur (S) battery as by far the most advanced electrochemical energy system for application in peak shaving/load leveling in the electric utility industry as well as for energy storage for distributed applications. Recently, NGK-TEPCO 2 MW NAS battery (16 MWH capacity) was installed at American Electric Power (AEP) site. It has a proven charge/discharge (roundtrip) efficiency of ~90% (90% of the stored energy can be recovered for use; i.e. only about 10% loss). At the present time, the installed capacity exceeds 60 MW (480 MWh with a 8 hour discharge), with systems as large as 8 MW, capacity as large as 64 MWh, with demonstrated life in excess of 7 years, safety has been demonstrated through rigorous testing, and the projected cost (for over 400 MWh/year) of $140/kWh. In addition, the Na-S battery can be readily integrated with a number of power generation systems. However, the currently pursued Na-S battery is based on tubular BASE and thus is not as compact as desired, has some issues related to long term degradation associated with the sulfur cathode and glass seals, requires the use of expensive graphite to impart electrical conductivity to an otherwise insulating sulfur cathode, and if a cell fails, it fails with a high resistance (open circuit mode). Thus, if a cell fails in a series leg, the entire segment becomes ineffective. Also, the presence of sulfur makes it difficult to design a planar cell due to the issues related to seal corrosion. Thus, while there are many positive attributes to the Na-S battery, there also are important limitations.

This project is on electrochemical energy storage systems based on BASE, using novel cathodes, which are potentially far superior to sulfur and overcome the above-stated limitations. Also, the pursued concept is on both tubular and planar cells using high strength and highly (ionic) conducting BASE plates, made using a novel, vapor phase process. The BASE made using this process exhibits strength as high as four times that of the state-of-the-art BASE, with obvious implications concerning reliability. This BASE is also resistant to water attack, unlike the BASE made by the conventional process. The cathodes investigated in this work are certain salts of nontoxic metals and the electrochemical energy storage (discharge) relies on displacement reactions. The attributes of these cathodes are as follows: (a) They are completely benign. Thus, their disposal is not problematic. (b) They give, with Na as the anode, an open circuit voltage (OCV) of (~2 V) or greater (~2.4 V), which is greater than Na-S system. (c) They do not corrode any of the materials of construction, such as steels, which makes it possible to use inexpensive materials and construct planar, series-connected, compact stacks. (d) The cathode is liquid over a wide temperature range, and exhibits excellent electrical conduction properties, which allows for much greater depths of discharge (high specific

energy) than possible with the Na-S system. (e) High electrical conductivity of the cathode implies that low resistance shunt forms, if a cell fails. Thus, if one cell fails the rest of the cells in a series leg continue to function normally and deliver power. (f) No graphite is required in the cathode. (g) Cells can be assembled in a fully discharged state. Thus, it is not necessary to handle metallic sodium, simplifying assembly procedure. (h) None of the materials are expensive. Thus, the projected cost of the system will be lower than the Na-S system, which is already expected to be cost-competitive with other energy storage systems and with proven reliability and availability.

The subject electrochemical system can operate over a wide temperature range, from 300 to ~600^{o}C, unlike the Na-S battery. Thus, it can be thermally integrated with many power generation systems, such as intermediate temperature or high temperature solid oxide fuel cells (SOFC). In this project, single cells were made and electrochemically characterized. Electrochemical and microstructural characterization techniques were used to examine the materials and cells, before and after testing.

This report describes the results of work conducted during the period September 1, 2005 and May 31, 2007. The results include the following: (1) Fabrication of sodium beta" alumina solid electrolyte (BASE) using a vapor phase process. (2) Characterization of BASE by X-ray diffraction, and conductivity measurements. (3) Kinetic studies on the conversion of α-alumina + YSZ into BASE + YSZ, and the effect of microstructure. (4) Ion exchange studies in $ZnCl_2$, $SnCl_2$ and SnI_4 as potential cathode materials. (5) Fabrication of planar and tubular BASE. (6) Design, construction and electrochemical testing of a symmetric cell containing BASE as the electrolyte and NaCl + $ZnCl_2$ as the electrodes. (7) Design, construction, and evaluation of Na/BASE/$ZnCl_2$ electrochemical cells. (8) Conducting several charge-discharge and several thermal (freeze-thaw) cycles. (9) Preliminary work on the assembly and testing of a two cell stack. (9) An assembly of a 5 cell stack. (10) Preliminary evaluation of the effect of porous surface layers on cell resistance.

EXPERIMENTAL

(1) Fabrication of BASE discs and tubes by the vapor phase process:

(i) Fabrication of BASE discs and tubes by powder pressing, sintering followed by vapor phase conversion:

In order to fabricate BASE discs by the vapor phase process, the starting materials used were CR 30 (Baikowski International Corporation, high purity $\alpha - Al_2O_3$) and TZ – 3Y (Tosoh corporation, 3 mol.% Y_2O_3- partially stabilized tetragonal zirconia). To ensure good dispersion of the powder mixture in water, a pH test was conducted. For this test, aqueous solutions ranging in pH from 1 to 11 were made using dilute HNO_3 and dilute NH_4OH in DI water. The powder mixture was added to each of the different pH solutions, stirred using a high frequency sonicator and allowed to settle overnight. The powder was found to be well dispersed in the solution with pH ~ 10. Then, 70% by volume of CR 30 and 30% by volume of TZ – 3Y were dispersed in the pH 10 solution and dried. The powder mixture was then ball milled with ethanol for 8 hours. The dried powder was ground, sieved and compacted to form circular discs by die – pressing uniaxially at 10,000 psi. The discs were then isostatically pressed at 30,000 psi. The samples were heated at 4^oC/min in air to 1600^oC and maintained at temperature for 1 hour and subsequently furnace cooled to room temperature. The density of the sintered samples was > 99% of the theoretical density.

In order to convert the α-Al_2O_3/ TZ–3Y discs to β" alumina (BASE), the samples were packed in a BASE packing powder in a ceramic 4-YSZ crucible and heat treated at elevated temperatures, typically 1450^oC. This BASE powder was prepared separately using the following procedure. Its composition was as follows: 8.7% (wt.) of Na_2O, 0.7% (wt.) of Li_2O and 90.6% (wt.) of α-Al_2O_3. The powder was ball milled in ethanol overnight and then dried. The dried powder was calcined at 1250^oC for 6 hours. The sintered samples were packed in the BASE packing powder containing excess 5% $NaAlO_2$ and heat treated at 1450^oC for 2 hours. X-ray diffraction patterns of the as-sintered and converted samples were obtained and various peaks were identified.

A few samples were mounted in an epoxy for analysis under optical and scanning electron microscopes (SEM). The surface quality and defects of BASE discs were examined under a "Nomarski" microscope in cross-polarized light. Surface microstructure and phases present in the BASE discs were analyzed using SEM.

BASE one end closed tubes were also made for electrochemical tests. These tubes were subsequently used for electrochemical tests on symmetric (same both electrodes) and asymmetric Na/BASE/$ZnCl_2$ cells. For the fabrication of BASE tube by isostatic pressing, the powder mixture in the required proportion of α-Al_2O_3 and TZ-3Y was introduced into a tubular polyurethane mold and was isostatically pressed at 30,000 psi. The green tubes were removed from the mold, heated at a rate of 3^oC/min to 1600^oC, and

maintained at temperature for 1 hour by placing each tube vertically in a ceramic crucible using a coarse α-Al_2O_3 & 3YSZ powder mixture to hold the tubes in place. The sintered tubes were converted to BASE by packing them in BASE powder in a crucible, heating in air to 1450^{o}C, and maintaining at temperature for 2 hours.

(ii) Fabrication of BASE discs by tape casting, sintering followed by vapor phase conversion:

To reduce the ohmic area specific resistance (ASR), the BASE plates should be as thin as possible while maintaining sufficient strength. In order to fabricate thin and flat BASE plates, tape casting was also used, in addition to die pressing. The BASE discs were fabricated using the vapor phase process with the starting materials as CR 30 (Baikowski International Corporation, high purity $\alpha - Al_2O_3$) and TZ – 3Y (Tosoh corporation, 3 mol.% Y_2O_3- partially stabilized tetragonal Zirconia). To ensure maximum dispersion of the powder mixture, a solution with pH ~10 was used as the solvent. 70% by volume of CR 30 and 30% by volume of TZ – 3Y were dispersed in the pH~10 solution and dried. It was then ball milled in ethanol for 8 hours. The dried powder was ground and sieved. To make the tape cast slip, the binders used were B-98, S-160, PAG and KD – 1 with ethyl alcohol and methyl ethyl ketone as solvents. The mixed powder and the binders and solvents were mixed in required proportions and ball milled for 6 hours. The slip was then filtered, de-aired and cast into a thin sheet. After the cast was dried, it was laminated and punched into circular discs of diameter 2.5". These discs were heated to 1000^{o}C for 2 hours, ramping up at a rate of 0.1^{o}C/min up to 450^{o}C and 2^{o}C/min up to 1000^{o}C and cooling down fast. The samples were heated at 4^{o}C/min in air to 1600^{o}C and maintained at that temperature for 1 hour and subsequently cooled at the same rate. The samples were then creep flattened and converted to BASE.

In order to convert the α-Al_2O_3/ TZ–3Y discs to β" alumina (BASE), the same procedure as described above was used. The BASE discs obtained had a thickness of 0.8 mm.

X-ray diffraction patterns of the as-sintered and converted samples were obtained and the various peaks were identified. The microstructures of the unconverted and BASE discs were obtained using SEM. A few BASE samples were put in an aqueous solution of NaOH (40(w/v) %) and boiled for 5 hours. This test was conducted to make sure that the samples would survive in an aqueous basic environment. This is to determine stability in aqueous NaOH environments for possible electrochemical devices based on this novel, moisture-resistant BASE. The X-ray diffraction patterns and microstructures of the samples after treating with NaOH were also taken and compared.

(iii) Fabrication of BASE tubes by slip casting, sintering followed by vapor phase conversion:

BASE one end closed tubes were also made for electrochemical tests. These tubes were subsequently used for electrochemical tests on symmetric (same both electrodes) and asymmetric Na/BASE/$ZnCl_2$ cells. For the fabrication of thin BASE tubes, the method of slip casting was used. The powder mixture in the required proportion of α-Al_2O_3 and TZ-

3Y was mixed with DI water and 2.5 (wt) % DARVAN C (dispersant). The solids loading used was 70%. The mixture was ball milled for 2 hours and de-aired for 10 minutes. The slip was then poured into the molds and after a residence time of about 1 minute, the slip was poured out of the mold. After the molds were dried, the green tubes were removed from the mold and heated at a rate of 3^{o}C/min to 1600^{o}C, and maintained at that temperature for 1 hour by placing each tube vertically in a ceramic crucible using a coarse α-Al_2O_3 & 3YSZ powder mixture to hold the tubes in place. The sintered tubes were converted to BASE by packing them in BASE powder in a crucible, heating in air to 1450^{o}C, and maintaining at temperature for 2 hours. The BASE tubes thus obtained were of thickness 1 mm.

(2) Characterization of BASE by X-ray Diffraction (XRD), Impedance Spectroscopy and Na-Na cells:

XRD patterns were obtained of the as-sintered α-alumina + zirconia samples as well as after conversion to beta"-alumina + zirconia. Impedance spectra were obtained over a range of temperatures from 300 to 500^{o}C. Typically, platinum paste electrodes were used. In a few cases, fiber glass filter papers impregnated with $NaNO_2$-$NaNO_3$ eutectic backed by Pt foils were used as electrodes. Measurements of conductivity on select tubes samples were conducted using sodium-sodium cells. The procedure used for conducting impedance spectroscopy is described in what follows.

Electrochemical impedance spectroscopy was conducted on a BASE disc to calculate the resistivity of the sample. Platinum paste was applied on either side of the sample and sintered at 1000^{o}C. Platinum wires of 0.25 mm diameter were used as the electrical leads. The whole fixture was placed in an alumina tube and inserted into a tube furnace for impedance analysis. A thermocouple was placed near the sample for temperature measurement. Impedance analysis was conducted at different temperatures ranging from 350^{o}C to 500^{o}C in 50 degree intervals. Solartron 1287 Electrochemical interface and Solartron 1260 potentiostat were used for impedance spectroscopy. In order to obtain the resistance of the sample alone, the test was repeated without the sample, with only the platinum wires connected to one another after removing the sample from the fixture.

(2-a) Kinetics study of Conversion of Alpha-Alumina + Zirconia into Sodium Beta" – Alumina + Zirconia:

The objective of the kinetic study was to determine the temperature – time – density as well as temperature – time - grain size relation. For this, a mixture of 70 vol.% α-Al_2O_3 and 30 vol.% 3–YSZ (CR–30 and TZ-3Y, respectively) was prepared by planetary milling to ensure a well-mixed, fine starting powder. Several α-alumina/3YSZ discs were prepared by die pressing followed by isostatic pressing. These samples were then sintered at different temperatures and durations: temperatures ranging from 1500^{o}C to 1800^{o}C and duration from 1 hour to 4 hours. The densities of these samples were determined.

The samples sintered at different temperatures were fine – polished, thermally etched and analyzed under a Scanning electron Microscope to determine the grain sizes of the

samples. These samples were then converted to sodium β" – alumina/ 3YSZ by heat treating those at different temperatures – 1250°C, 1300°C, 1350°C, 1400°C and 1450°C and durations ranging from 30 minutes to 15 hours. Conversions at 1250°C and 1450°C were started with the smallest grain size samples. As the conversion kinetics is different for different converting temperatures, the ranges of duration will also change accordingly: lower conversion temperature having longer duration. The converted samples were cross sectioned, coarsely polished and analyzed again under Scanning Electron Microscope to measure the thickness of the sample converted thereby calculating the corresponding conversion rates.

(3) Theoretical model:

A preliminary theoretical model explaining the conversion kinetics of α – alumina/3YSZ samples to sodium β" – alumina/3YSZ samples was proposed. The conversion was done using a patented vapor phase method and the chemical reaction is as follows:

$Na_2O + \sim 6Al_2O_3 \rightarrow Na_2O.\sim 6Al_2O_3$ (β")

The conversion takes place by the coupled transport of Na^+ ions and O^{2-} ions through the ceramic. Sodium β" – alumina is a good conductor of Na^+ ions. However, to convert α into β", it is necessary to incorporate Na_2O. Thus, both, Na^+ and O^{2-} should have reasonable diffusivities. In order to facilitate faster conversion, an alternative path was provided for the oxygen ions by making the starting ceramic a composite of α – alumina and 3 YSZ where YSZ is a good oxygen ion conductor. Initially, a thin layer of sodium β" alumina will be formed on the surface of the ceramic. Sodium ions will be conducted through this layer of β" alumina and oxygen ions will be conducted through YSZ layer. The kinetics of conversion may be either interfacial controlled or diffusion controlled or a combination of both. When the thickness converted is small, the kinetics will be linear (interfacial controlled) and when the thickness converted is large, the kinetics will be parabolic (diffusion controlled). The process of conversion to sodium β" alumina can be broken down to three steps: Interface reaction at the three phase boundary, transport of ions across the bulk and formation of Na_2O at the reaction interface. Figure 2 shows a schematic.

Assuming Quasi Steady state:
$Na_2O \qquad 2Na^+ (\beta") + O^{2-} (YSZ)$

As there is no external field applied, the electric current in the circuit should be zero

i.e. $J_{Na+} = 2 J_{O^{2-}}$

Assuming quasi steady state:
$J^I_{Na2O} = J_{Na2O} = J^{II}_{Na2O}$

At the interface I
$J^I_{Na2O} = K^I (\mu^I_{Na2O} - \mu'_{Na2O})$

At the interface II
$J^{II}_{Na2O} = K^{II} (\mu"_{Na2O} - \mu^{II}_{Na2O})$

$dx \alpha J_{Na2O}\, dt$

General form of the equation derived:
$\mathbf{X^2(1/D_{eff}) + X(1/K_{eff}) - (X_o/D_{eff} + 1/K_{eff})\, X_o = t}$

Time t is defined as the hold time at the conversion temperature. So at t = 0, there will be an initial thickness converted (Xo) as the conduction of ions takes place even during the heating up process.

When the conversion thickness (x) is small
Interface controlled reaction (Linear Kinetics)
$\mathbf{X/Keff = C_1 t}$

When the conversion thickness (x) is large
Diffusion controlled reaction
$\mathbf{X^2/D_{eff} = C_2 t}$

(4) Measurement of BASE tube conductivity:

An experiment performed was to determine the conductivity of the BASE tube. For this experiment, a symmetric cell was used. From the phase diagram of NaCl – $ZnCl_2$, it was found that a eutectic is present at 262^{o}C with 71 mol. % $ZnCl_2$ [1]. The experimental set up was placed inside an argon filled glove box with the configuration given below.

$$Zn \mid ZnCl_2 + NaCl\ (eutectic) \mid BASE \mid ZnCl_2 + NaCl\ (eutectic) \mid Zn$$

The BASE tube was placed in a glass test tube. A eutectic mixture of NaCl and $ZnCl_2$ with Zn metal turnings was melted. The inside and outside of the BASE tube were filled with the molten salt and zinc electrodes were placed in the molten salt. The cell was placed within a small tube furnace and heated to 350^{o}C. The temperature was controlled using a thermocouple placed outside the glass tube. Voltage and current leads were connected to the Zn electrodes. The cell was then cycled in constant current mode supplying 500 mA for 50 hours.

(5) Na/$ZnCl_2$ Electrochemical Cell Construction: Electrochemical cell can be assembled in one of three states: discharged state, charged state and partially charged state at eutectic composition.

- Discharged state: If the cell is constructed in the discharged state the advantage is that there is no need to handle metallic sodium. In the discharged state, the salt mixture (NaCl + $ZnCl_2$) is placed outside the BASE tube (inside a glass tube). During charging, sodium transports through the BASE tube and eventually fills up the tube. However, in this state zinc metal must be added to the positive electrode and be electrochemically available which implies that it should be in contact with

the electrode during charge. When in contact with the electrode, the electrons formed by the ionization of Zn metal will conduct through the electrode easily. A possible disadvantage is that the required salt composition for operation at 375^{o}C, if solidified after melting, may not be homogenous until heated above 400^{o}C. One approach is to use steel wool or felt, in which metal and/or salt can be retained.

- Charged state: The cell constructed in the charged state will have pure $ZnCl_2$ on porous substrate as the positive electrode. No zinc is required at the positive electrode. The BASE tube is filled with sodium. The disadvantage is that it is necessary to handle metallic sodium and the BASE tube must be completely wet by the sodium metal.
- Partially charged state at eutectic composition: The advantage of this method is that the eutectic composition melts at the lowest possible temperature (262^{o}C). It is easy to melt and there is no problem of segregation. However, in this construction, both metallic sodium and zinc need to be incorporated in the cell during assembly.

(5-a) Investigation of the Stability of BASE in $ZnCl_2$: An experiment was conducted to test the stability of BASE in zinc chloride environment. Two BASE tubes were used for these tests. Tubes were thoroughly cleaned and dried in an oven. Both were weighed separately. The weight of the first tube was 10.386 g and that of the second tube was 7.320 g. The samples were then soaked in molten zinc chloride at a temperature of 430^{o}C for 22 hours. These tests were conducted inside a glove box. After 22 hours, the samples were removed, cleaned and dried. The samples were then weighed and analyzed using a Scanning Electron Microscope. The objective of this experiment was to determine if Zn^{2+} can replace Na^{+} by ion exchange. It is necessary that negligible ion exchange occur. If some ion exchange occurs, then it is necessary that this doe not lead to cracking of the BASE. It is known that in BASE, those ions which are monovalent and of nearly the same size as Na^{+} tend to ion exchange. The ion which readily replaces Na^{+} is Ag^{+}, the latter being a highly polarizable ion. Zn^{2+} is much smaller than Na^{+}. Thus, it was the expectation that ion exchange should not occur.

(5-b) Ion exchange experiments with Tin (II) Chloride and Tin (IV) Iodide:

As stated in the original proposal, the potential cathode salts also include Sn-based salts. The potential salts are divalent Sn salts and tetravalent Sn salts. The ionic radius of Sn^{2+} is close to that of Na^{+}, but that of Sn^{4+} is much smaller. Thus, we expect greater tendency for ion exchange with divalent Sn salts. The objective of this experiment was to explore the ion exchange characteristics. In order to conduct the ion exchange experiments, die pressed samples were used. The samples were washed and dried in the oven at 300^{o}C for 2 hours. The samples were weighed on a sensitive balance. One of the samples was packed in Tin (II) Chloride in a crucible and heated at 300^{o}C. The sample was soaked for 20 hours. It was then washed thoroughly and dried in an oven as before. The sample was weighed again. Another sample was packed with Tin (IV) Iodide in a crucible and heated to 160^{o}C and maintained at temperature for 24 hours. The experiment with SnI_4 was conducted at a lower temperature since SnI_4 is not stable at higher temperatures. Based on other work on ion exchange, it was deemed that still ion exchange may occur if the

thermodynamics and kinetics were favorable. After washing thoroughly, the sample was dried in the oven and weighed as before. Chemical line scan was conducted using a Scanning Electron Microscope for analyzing the composition of the samples.

(6) Electrochemical cell with BASE tube as electrolyte:

The objective of this experiment was to test the electrochemical working of a cell with a BASE tube as electrolyte (i.e. Na/BASE/$ZnCl_2$). Testing of tubular cell is easier as this can be readily easily done inside a glove box with minimal of preparation. The cell was assembled in the fully discharged state. The volume of the BASE tube was calculated to be 5 ml. The amount of salt required to obtain approximately 5 ml of sodium was determined from the chemical reaction as follows:

The actual reaction during discharge is

$$2Na + ZnCl_2 \rightarrow 2NaCl + Zn$$

As the cell was to be started in the fully discharged state, the direction of reaction during charging would be from right to left. As per the phase diagram, the eutectic composition is 55 mol. % $ZnCl_2$ and 45 mol. % $(NaCl)_2$. Then the reaction would become,

$$2Na + 2.22ZnCl_2 \rightarrow 1.22ZnCl_2 + (NaCl)_2 + Zn$$

The electrochemical cell was constructed by placing a cylindrical electrode of stainless steel into a glass test tube of outer diameter 25 mm. Zinc sheet rolled into a cylinder was placed inside and in contact with a cylindrical steel electrode. An aluminium pin of approximately the same dimensions (slightly smaller) as that of the BASE tube was inserted and "0" grade steel wool was wedged into the annulus. This steel wool was degreased and cleaned before inserting into the tube. After removing the metal pin, the required quantities of salts (16.63 g $ZnCl_2$ and 11.69 g NaCl) of previously fused and ground salt of composition 1.22 $ZnCl_2.(NaCl)_2$ was added to the glass tube. The bottom of the tube was heated in a furnace after evacuation and back filling with Argon. The temperature was raised to ~420^oC. The sealed tube was then cooled, transferred to the glove box and reheated up to 400^oC to insert the BASE tube sealed to the alumina tube through the hole in the steel wool and into the molten salt. Prior to the insertion of BASE tube, degreased steel wool of grade 000 was stuffed inside the BASE tube and copper wire was inserted as the negative electrode. The open end of the alumina tube was connected to a copper tube with the help of an O – ring and the other end was compressed so that it would be sealed. Voltage and current leads were connected to the electrodes with the negative terminal connected to the copper wire and the cell was operated in the constant current mode.

(6-a) Electrochemical cell stack with BASE discs as electrolytes:

Three planar cells were assembled in the completely discharged state. Each cell was assembled separately and connected in series with the help of a stainless steel cylindrical block of diameter 1.5" and length about 1 inch. If these spacers were not used, the area of contact between the cells would have been lower, resulting in an increase in resistance, thereby increasing the voltage loss associated with it. The three–cell stack was then placed in a tube furnace inside the glove box. The effective cell area of each cell was about 11.3 sq.cm. The cathode of each cell contained 5.85 g NaCl, 6.82 g $ZnCl_2$ and 2 g Zn. The choice of the proportion of NaCl to $ZnCl_2$ was based on the available information on the phase diagram [1]. The amount of zinc added was not sufficient to fully utilize the available NaCl during charging. In the future, greater amount of zinc will be added to increase the capacity. Voltage and current leads were connected to the stainless steel electrodes with negative terminal connected to the upper end plate of the top cell and positive terminal connected to the lower end plate of the bottom cell. The cell stack was charged in a constant current mode at a temperature of 400^oC.

(6-b) Construction of a planar cell stack:

A planar cell stack of five cells was constructed. The cells were assembled in a fully discharged state. Two stainless end plates with cavities were used on either ends of the stack assembly. Stainless steel (SS) rings were stacked separated by SS foils. Copper gaskets were used to form a good seal between the BASE disc and the SS rings. These five cells were connected in series with the help of bolts, nuts and washers. Alumina sleeves were provided on the bolts for electrical insulation between the cathode and anode of the same cell. Thin SS strips were attached on both end plates as terminals. The salt mixture was incorporated on the cathode sides of the cell stack as described above. Anode side had a thin film of sodium metal for initiating the charging by wetting the surface of the BASE electrolyte. To form a good contact between the sodium metal and the casing, '0' grade steel wool was stuffed in the anode cavities.

(7) Effect of Porous Surface Layers on Polarization: In solid oxide fuel cells (SOFC), it is well known that porous composite electrodes lower the polarization and improve performance. It was proposed in Phase I to investigate if porous layers will also improve performance of electrochemical devices made using BASE. Towards this end, BASE discs were fabricated with and without porous surface layers. These discs were tested in electrochemical cells using aqueous media. This was the approach taken to obtain some preliminary data. This approach also allowed us to explore if the vapor phase processed BASE, which is water-resistant, can actually be used in electrochemical cells in an aqueous environment.

(8) Fabrication of Sodium β" alumina electrolytes with embedded Platinum electrodes:

In order to fabricate BASE discs by the vapor phase process, the starting materials used were CR 30 (Baikowski International Corporation, high purity $\alpha - Al_2O_3$) and TZ – 3Y (Tosoh corporation, 3 mol.% Y_2O_3- partially stabilized tetragonal zirconia). Then, 70% by volume of CR 30 and 30% by volume of TZ – 3Y were dispersed in the pH 10

solution and dried. The powder mixture was then ball milled with ethanol for 8 hours. The dried powder was ground, sieved. The sieved powder was compacted to form a circular disc by die – pressing uniaxially at 10,000 psi and a thin radial strip of platinum paste was painted on the top surface of the green disc. A small square piece of filter paper was placed on top of the platinum strip. Another layer of powder was put of top of this disc and die – pressed uniaxially at the same pressure. Another platinum strip was painted as explained above with the filter paper on top of it. A third layer of disc was pressed and the three layers were compacted to form a single disc with two embedded platinum electrodes. The green discs were then heated at 1.5^{o}C/min in air to 800^{o}C and at 3.5^{o}C/min from 800^{o}C to 1600^{o}C and maintained at the temperature for 1 hour and subsequently furnace cooled to room temperature. The filter paper burnt off leaving a small gap to attach the platinum wires to the Platinum embedded strips. These samples were then converted to sodium β" alumina. In order to convert, the samples were packed in a BASE packing powder in a ceramic 4-YSZ crucible and heat treated at elevated temperatures, typically 1450^{o}C. This BASE powder was prepared separately using the following procedure. Its composition was as follows: 8.7% (wt.) of Na_2O, 0.7% (wt.) of Li_2O and 90.6% (wt.) of α-Al_2O_3. The powder was ball milled in ethanol overnight and then dried. The dried powder was calcined at 1250^{o}C for 6 hours. The sintered samples were packed in the BASE packing powder containing excess 5% $NaAlO_2$ and heat treated at 1450^{o}C for 2 hours.

(8-a) Fabrication of Sodium β" alumina electrolytes with embedded Carbon fibers:

The powder for the fabrication of BASE discs was prepared as explained above. The sieved powder was compacted to form a circular disc by die – pressing uniaxially at 10,000 psi and a thin carbon fiber of diameter 75 μm was placed radially starting from the center of the disc. Another layer of powder was put of top of this disc and die – pressed uniaxially at the same pressure. On top of the second layer, another carbon fiber of same radius and length as before was placed radially. A third layer of disc was pressed and the three layers were compacted to form a single disc with two embedded carbon fibers. The green discs were then heated at 1.5^{o}C/min in air to 800^{o}C and at 3.5^{o}C/min from 800^{o}C to 1600^{o}C and maintained at the temperature for 1 hour and subsequently furnace cooled to room temperature. The carbon fibers were burnt off leaving two radial holes running from the center to the edge. These samples were then converted to sodium alumina. In order to convert, the samples were packed in the special BASE packing powder as before, in a ceramic 4-YSZ crucible and heat treated at elevated temperatures, typically 1450^{o}C.

RESULTS AND DISCUSSION

X-Ray Diffraction: Figure 2 shows an x-ray diffraction (XRD) pattern of an as-sintered α-alumina + zirconia disc sample before converting to BASE. The discs were formed by isostatic pressing of powder mixtures. The XRD shows the presence of the two phases; α-alumina and zirconia. Figure 3 shows an XRD pattern of the sample after conversion to BASE. In Figure 2, the peaks were identified to be those of α-Al_2O_3 and YSZ. In Figure

3, the peaks corresponding to BASE and YSZ can be seen. No peaks corresponding to α-alumina are present indicating complete conversion of α-alumina into BASE. Conversion experiments were also conducted on tape cast α-alumina + 3 YSZ. Figure 4 shows an XRD trace of as-sintered (tape cast) sample. Figure 5 gives an XRD trace of the sample after conversion to BASE. These results demonstrate that BASE can be formed by the vapor phase process using either isostatic pressing or slip casting of α-alumina + YSZ as the method of green forming. This means in both methods, α-alumina and YSZ phases were contiguous. Figure 6 is an SEM image of the as-sintered sample. The light grains are of YSZ and the dark grains are those of α-alumina. Figure 7 is an SEM image of the sample after conversion to BASE. Note the slight change in morphology as α-alumina converts into BASE.

Sintering Conditions, Microstructure Development: It is known that the ionic conductivity of BASE is a function of grain size; the larger the grain size, the higher the conductivity. In the vapor phase conversion process, the approach to making samples of varying grain sizes involves first fabricating samples of α-alumina + zirconia of various grain sizes by varying the sintering conditions (temperature and time). The sintered samples then are subjected to vapor phase conversion, resulting in BASE samples of differing grain sizes. The kinetics of conversion is expected to depend upon the grain size. This part of the work focused on the investigation of the kinetics of conversion.

Figures 8 and 9 show the microstructures of two samples with widely differing grain sizes. The average grain sizes of the samples were determined. Table 1 shows grain size as a function of sintering conditions. The grain size (average of alumina and zirconia) of the sample sintered at 1500^{o}C/1 hour was 0.53 $\pm$ 0.031 μm and that of the sample sintered at 1800^{o}C/1 hour was 2.7 $\pm$ 0.056 μm. The growth in grain size was about 5 times when the temperature was increased from 1500^{o}C to 1800^{o}C. This result is as expected since the sample sintered at higher temperature and for longer time exhibits a larger grain size.

The above mentioned samples were then converted to sodium beta"-alumina at temperatures of 1300^{o}C, 1350^{o}C and 1400^{o}C for different hold times ranging from 30 minutes to 15 hours. The samples were cross sectioned, coarse-polished and analyzed to determine the rate of conversion from α-alumina to β"-alumina. Samples of smaller grain sizes were converted at 1250^{o}C and the samples are yet to be analyzed under the scanning electron microscope. Figures 10, 11 and 12 show the plots of thickness converted as a function of hold time for different grain sizes. This result indicates that the rate of conversion is higher for the samples having smaller grain size. Moreover, the kinetics is initially linear followed by a parabolic kinetics with increasing thickness. Thus the theoretical model predicted was verified by the experimental results. Figure 13 shows the variation of conversion thickness of a particular grain size sample as a function of hold time at various conversion temperatures. The conversion kinetics is shown only up to a hold time of 8 hours. This is due to the limitation of the thickness of the sample converted. For a hold time of 8 hours, the thickness converted at 1300^{o}C, 1350^{o}C and 1400^{o}C are of the order of 600 μm, 850 μm and 1380 μm, respectively. This result is as expected since the kinetics of conversion is proportional to the conversion temperature. Future work will include studying the kinetics of conversion at conversion temperatures

of 1250°C and 1450°C and fitting the theoretical model with the experimental data to determine various parameters.

Table 1: Grain size as a function of sintering conditions

Sintering Temperature (°C)	**Hold time (hours)**	**Grain Size (um)**
1500	1	0.53 ± 0.031
1500	2	0.57 ± 0.045
1500	4	0.61 ± 0.052
1550	1	0.67 ± 0.003
1550	2	0.74 ± 0.051
1550	4	0.86 ± 0.077
1600	1	0.95 ± 0.013
1600	2	1.14 ± 0.026
1600	4	1.32 ± 0.029
1700	1	1.80 ± 0.023
1800	1	2.70 ± 0.056

These results can be explained in terms of transport mechanisms. Over the range of conversion thicknesses studied, which are well over 1 mm, it is observed that the kinetics is initially linear and becomes parabolic as the conversion thickness increases. It is clear that the kinetics is thermally activated as well from Figure 13.

The observation that the kinetics is linear implies the kinetics is not controlled by the parallel diffusion of Na^+ through the BASE formed and O^{2-} through the zirconia phase to the reaction front, even though conversion requires coupled transport of Na^+ and O^{2-}. At the reaction front, O^{2-} ions must transport through either the BASE formed, or through the α-alumina, or along the α-alumina/BASE interface. The diffusion distance is about half the grain size of α-alumina (or BASE). Since the grain size in a given sample is constant, the diffusion distance is fixed. This leads to the linear dependence (interface control) of conversion thickness on time, wherein the interface control parameter actually depends upon local diffusion. The three paths for diffusion are in parallel, and the phenomenon is very similar to the formation of pearlitic steel by a cellular decomposition of austenite in the iron-carbon system. As the diffusion distance is about half the grain size, the kinetics is slower in coarse-grained materials. Figure 14 shows a schematic of the mechanism of transport and conversion.

The observation that the kinetics is initially linear and follows a parabolic trend implies that the kinetics is controlled by two processes:

a) The interfacial reaction at the initial interface and at the reaction front where the O^{2-} ions are transported through either the BASE formed or through the α-alumina, or along the α-alumina/BASE interface.
b) Parallel diffusion of Na^+ through the BASE formed and O^{2-} through the zirconia phase to the reaction front

When the thickness converted is small, the coupled transport of both the ions will be faster compared to the interfacial reactions. Since the grain size in a given sample is constant, the diffusion distance of O^{2-} ions at the reaction front is fixed. This leads to the linear dependence (interface control) of conversion thickness on time, wherein the interface control parameter actually depends upon local diffusion. The three paths for diffusion are in parallel, and the phenomenon is very similar to the formation of pearlitic steel by a cellular decomposition of austenite in the iron-carbon system. As the diffusion distance is about half the grain size, the kinetics is slower in coarse-grained materials.

When the thickness converted is large, the interfacial reactions will be faster compared to the parallel diffusion of Na^{+} ions and O^{2-} ions, as the distance to be travelled is larger. As diffusion kinetics is parabolic, the conversion kinetics will show parabolic nature as well. Figure 14 shows a schematic of the mechanism of transport and conversion. A preliminary theoretical model was developed in order to explain the behavior of the electrolyte while conversion as a function of grain sizes and conversion temperature. Figure 15 shows the schematic of the kinetics of conversion.

Fabrication of BASE discs and tubes: Both powder pressing and tape casting/slip casting have been used as methods for green forming α-alumina + zirconia bodies. These have been then sintered and converted into BASE. Figure 16 shows a photograph of BASE discs made by tape casting followed by sintering and conversion. Figure 17 shows a photograph of a BASE tube made by slip casting followed by sintering and conversion.

Stability of BASE in Molten Salts: The battery concept proposed in Phase I involves molten sodium as the anode and salts such as $ZnCl_2$, $SnCl_2$, SnI_4, etc. as the cathodes. BASE is known to undergo ion exchange with a number of cations. The typical reaction is as follows

$$M^{z+}\text{-salt} + \text{Na-BASE} \rightarrow z\text{Na-salt} + M^{z+}\text{-BASE}$$

Where, M^{z+}-salt is a salt of M^{z+} cation with z+ as the valence. An example is

$$SnCl_2 + \text{Na-BASE} \rightarrow 2NaCl + Sn^{2+}\text{-BASE}$$

Na-BASE can undergo ion exchange reactions in many monovalent, divalent, and even trivalent cationic salts. Only those salts which do not undergo ion exchange to a significant extent can be used as cathodes for the battery. Extensive work has been reported with $NiCl_2$ and $FeCl_2$ as the cathodes, the so-called ZEBRA batteries. Negligible ion exchange occurs in these two salts. The objective of the present work was to determine the extent to which ion exchange occurs in $ZnCl_2$, $SnCl_2$, and SnI_4 salts.

Figure 18 shows an EDX scan of a BASE tube that had been immersed in molten $ZnCl_2$ salt for 22 hours at 430^{o}C. No weight change was detected. This is consistent with the observation that no ion exchange occurred.

Ion exchange experiments were also conducted in tin salts. A sample was packed in tin (II) chloride in a crucible and heated at 300^{o}C. The sample was soaked for 20 hours. It was then washed thoroughly and dried in an oven as before. The sample was weighed again. Figure 19 shows the line scan. It was noted that there was a net change in weight. The line scan showed that all of the sodium was replaced by tin, showing that ion exchange does indeed occur with Sn^{2+}. Also, the sample cracked due to the associated volume change. Another sample was packed with tin (IV) iodide in a crucible and heated at 160^{o}C for 24 hours. After washing thoroughly, the sample was dried in the oven and weighed as before. Chemical line scan was done using a Scanning Electron Microscope for analyzing the composition of the samples. As shown in Figure 20, no tin was found in the sample, indicating that no ion exchange occurred. These results show that while Sn^{2+}-salt is not suitable as a cathode, Sn^{4+} salt is a possible candidate. The two factors which determine whether or not Na^{+} ion can be replaced by ion exchange with another ion are the valence and the ionic size. The higher the valence, the lower is the tendency for ion exchange. Also, the greater the difference in ionic sizes, the lower is the tendency for ion exchange. Table 2 compares ionic radii of the various cations.

The table shows that Sn^{2+} is close to Na^{+} in size. The observed tendency for ion exchange suggests that the ionic size plays a major role. No ion exchange was observed with either Zn^{2+} or Sn^{4+}, which is attributed to their much smaller ion size compared to Na^{+}. In the case of Sn^{4+}, the large difference in valence is one more reason that ion exchange does not occur. The reported success of batteries with $FeCl_2$ and $NiCl_2$ thus must also be related to a greater difference in ionic sizes. Note also that Cu^{2+} salt should be a viable candidate, but not CuCl. Thus, in addition to $ZnCl_2$, the other possible candidates include SnI_4 and $CuCl_2$.

The observation that no ion exchange occurs with Sn^{4+} salt suggests that Sn^{4+} salt is a candidate as a cathode. With SnI_4 as the salt, at 600 K (227^{o}C), the free energy of the reaction

$4Na + SnI_4 \rightarrow 4NaI + Sn$

is ΔG^{o} = -928.531 kJ/mol with the corresponding open circuit voltage of 2.405 V. In Phase II, the viability of this cathode will be explored.

Table 2

Ion	Radius (A)
Na^{+}	1.16
Zn^{2+}	0.89
Fe^{2+}	0.92
Ni^{2+}	0.83
Sn^{2+}	1.05
Sn^{4+}	0.83
Cu^{2+}	0.87
Cu^{+}	1.08

Electrochemical Testing: Stability of BASE in $ZnCl_2$: Figure 21 shows the results of electrochemical testing of a BASE tube with NaCl + $ZnCl_2$ + Zn as the two electrodes. There was no evidence of increase in resistance with time. The BASE tube was weighed before and after the experiment and no change in weight was observed. This means no ion exchange (replacement of sodium ions by zinc ions in 2 to 1 proportion) occurred. That is, the displacement reaction between $ZnCl_2$ and the BASE tube did not take place. This is a very important result, and demonstrates the viability of the proposed concept. From the values of voltage and current obtained from the experiment, the resistance of the overall cell was calculated to be 0.15 Ω. This includes the resistance of the BASE tube, molten salts and the polarization resistance. The estimation of resistivity of the BASE tube from this test requires knowledge of the resistivity of the eutectic salt.

Electrochemical Testing of a Tubular Cell assembled in the fully charged state: Figure 22 shows the results of electrochemical testing (discharge only) of a tubular cell assembled in the fully charged state. Thus, sodium was introduced into the anode compartment (inside of the tube) and Zn + $ZnCl_2$ + NaCl in the cathode. Initially, a current of 50 mA was passed which was gradually increased to 250 mA in steps. After operating for 1 hour, the current was increased to 500 mA and the cell was discharged for about 2.5 hours with discharge voltage of about 2.0 V. The current was again increased to 1 A and the cell was discharged for another 2 hours with the output voltage of about 1.85 V. The cell was disconnected from the circuit without reducing the temperature and left overnight. An important observation is that the voltage was stable during discharge. This suggests that the voltage does not vary over a wide range of depth of discharge, a useful criterion from the standpoint of cell design. This means that the thermodynamic activity of sodium in the cathode remains rather low over a large depth of discharge (activity of sodium in the anode is unity). Note that the OCV is well over 2 V and a significant current (500 mA) could be drawn at a high voltage (2 V).

Fabrication of Planar cells: Figure 23 shows the cathode side and the anode - electrolyte assembly of planar cells. Cathode side includes a copper crucible with a copper wire attached to it. Copper wool is filled in the crucible in which the molten salt was poured. Anode side consists of an alumina crucible with a hole in the middle which is attached to the BASE disc. A copper wire is inserted in the hole, once molten sodium is filled in the anode container. A smaller version of the same anode construction is also shown. This was made with a 1" diameter BASE disc as electrolyte.

Figures 24 (a), (b) and (c) show the voltage response of the charge discharge cycles of a planar cell assembled in the partially charged state at the eutectic composition. Figures 24 (b) and (c) show the voltage response after one and two freeze thaw cycles respectively. The cell was operated for about 2 hours each time. From the voltage response, it could be inferred that the planar cells can withstand several freeze thaw cycles without any electrolyte failure. The open circuit voltage obtained was about 2.35 V. The cell was operated at a constant current of 100 mA and at a temperature of 350^{o}C. In the case of the planar cell, the duration of discharge is low as compared to that of tubular cells due to the smaller amounts of electrode materials used. The discharge cycle was shorter in the

planar cell as there was only a small amount of sodium (0.9 ml) in the anode side. As no copper wool was used in the anode side, the cell resistance was somewhat higher. This is due to the non - uniform wetting of sodium on the BASE disc, but can be easily addressed. Specifically, the addition of a small amount of sodium amide is known to improve wetting.

Figure 25 shows a photograph of the insides of a planar cell made using stainless steel fixtures. The planar cell was assembled in a fully discharged state. The electrolyte was positioned at the center using a steel wire–alumina ring. The charging and discharging of this cell was done at a temperature of 425^{o}C, which is above the melting point of zinc. This cell was operated for about 50 hours. Figure 26 shows the voltage response of charge – discharge cycles of the planar cell. A constant current of 100 mA was initially passed through the cell for 5 hours which was increased to 200 mA. The cell was cycled at 250 mA for 13 hours. Later, the charging current was gradually increased to 500 mA and was operated for another 32 hours. For the sake of clarity, Figure 26 shows only a part of the voltage response of the cell (for 20 h). The planar cell did not fail even after operating it for over 50 hours at a temperature of 425^{o}C.

Construction and Electrochemical Testing of a Planar Three Cell Stack: In Phase I, the objective is to demonstrate a planar stack. The most expedient approach was to stack individual cells of the type shown in Figure 25. In Phase II, effort will be devoted to minimizing the stack volume and mass by minimizing the volume and mass of passive components (e.g. end plates) and maximizing the reactant volume and mass to increase specific power and specific energy. Figure 27 shows a photograph of a three cell stack assembled using cells of the type shown in Figure 25. One of the cells was shorted due to leakage from the sides. The remaining two cell stack was charged. The results are shown in Figure 28. Note that the net cell voltage at 100 mA charge current is in excess of 4 V.

Design and Assembly of a Five Cell Stack: Figure 29 shows a 5 cell planar stack using improved design.

The Role of Surface Texture of BASE on Electrochemical Performance: Experiments using an Aqueous System: In solid oxide fuel cells (SOFC), it is well known that electrode microstructure play a key role in reducing polarization. In SOFC, the electrochemical reaction involves three phases; gas phase, electrode, and electrolyte. In composite electrodes, the reaction occurs at three phase boundaries (TPB). Porous layers enhance the TPB, and this is routinely used in SOFC. In the batteries under study here, the electrochemical reaction involves two phases (no gas phase). Even then surface texture is expected to improve performance; and this task was proposed as part of Phase I work. BASE discs with and without porous surface layers, were fabricated. For the Phase I work, experiments in aqueous system were not proposed. However, it was decided to conduct experiments in aqueous systems since this achieved two objectives. (1) This allowed the investigation of the effect of porous surface layers on performance using simple tests without elaborate high temperature testing. (2) This also facilitated the demonstration of the exceptional resistance of the vapor phase processed BASE to moisture attack.

Figure 30 shows an electrochemical cell constructed with BASE discs. One electrode contained a metallic zinc (sponge) mixed with an aqueous solution of $ZnCl_2$ and NaCl. The other electrode contained metallic copper (sponge) mixed with an aqueous solution of $CuCl_2$ and NaCl. This is effectively a Daniel Cell.

During discharge, the reaction at the anode is:

$Zn + 2NaCl \rightarrow ZnCl_2 + 2Na^+ + 2e'$

$2Na^+$ transport through BASE to the cathode, and 2e' transport through the external circuit to the cathode.

The reaction at the cathode is:

$2Na^+ + 2e' + CuCl_2 \rightarrow 2NaCl + Cu$

The net cell reaction is

$Zn + CuCl_2 \rightarrow ZnCl_2 + Cu$

This is achieved by transporting sodium ions through BASE.

Experiments were conducted using two discs of BASE, one without and one with porous surface layers. Figure 31 shows charge-discharge characteristics of the cell without porous surface layers. Figure 32 shows charge-discharge characteristics of the cell with porous surface layers. Note that the net cell resistance is considerably lower when porous layers are present. Note also that electrochemical devices can be envisioned in aqueous media using the water resistant BASE made by the vapor phase process, which is not possible with BASE made using the conventional process.

Sodium β" alumina with embedded Platinum electrodes: Figure 33 shows the sodium β" alumina samples with platinum electrodes embedded and Platinum wire attached to it. The electrolyte discs were successfully sintered. However during the conversion process the electrolytes got delaminated.

Sodium β" alumina with embedded Carbon fibers: The electrolyte discs were successfully sintered. However during the conversion process the electrolytes got delaminated. 1 wt% ceramic binder (Poly Vinyl Butyral) was used in order to prevent any delamination of the solid electrolyte during conversion. During conversion, the electrolyte was delaminated in spite of the ceramic binder. As the conductivity of Na^+ ions in the air is negligible, the transport of the ions will be blocked leading to the delamination of the ceramic while conversion. In the future, the electrolyte discs will be sintered and converted to sodium alumina without making any layers and equally spaced micro holes of diameter 100 μm will be drilled using precision machining techniques. Figure 34 shows the top view and side view of the electrolyte disc with two micro holes

drilled radially. Thin Platinum wires will be threaded into these holes which will act as embedded electrodes. Electrochemical testing will be done using these electrolytes with threaded Platinum wires to determine the chemical potential profile of Na^+ ions across the BASE.

CONCLUSION

(1) BASE could be successfully fabricated using a vapor phase process. (2) BASE tubes and discs were fabricated for various types of electrochemical cells. (3) The kinetics of the conversion process was investigated with emphasis on the effect of microstructure on conversion kinetics. (4) Ion exchange studies were conducted in $ZnCl_2$, $SnCl_2$, and SnI_4. It was observed that no ion exchange occurred in $ZnCl_2$ and SnI_4, but did occur in $SnCl_2$. This suggests that $ZnCl_2$ and SnI_4 are potential cathodes. (5) Electrochemical cells were constructed with Na anode, BASE electrolyte and $ZnCl_2$ as the cathode. (6) Cells were successfully subjected to several charge-discharge, and freeze-thaw cycles. (7) A roundtrip efficiency of ~88% was measured at reasonable current levels. With increased BASE conductivity, even higher values are expected. (8) Cells were operated successfully at temperatures as high as 425^{o}C, with expectations of operation at even higher temperatures. (9) A two cell planar stack was assembled and successfully tested. (10) A five cell stack was assembled.

REFERENCES

[1] 'Phase Diagrams for Ceramists: Volume II', a publication of the American Ceramic Society, Westerville, OH (1969).

COST STATUS

The total budget for 2 years (24 months)	$499,998.00
The DOE portion:	$399,998.00
The University of Utah Cost Match	$100,000.00
Total Amount Spent Through March 31, 2008	$499,998.00

This consists of graduate student stipend, the PI salary (partial), supplies, and the use of equipment (XRD, SEM).

SCHEDULE STATUS

No specific milestones were identified in the Phase I proposal. However, the work has progressed on the following tasks, and work is on schedule.

Task 1.0: Fabrication of BASE plates by a vapor phase process. BASE plates made by tape casting. Also made are BASE tubes by slip casting.

Task 2.0: Fabrication of metal end caps for planar cells. End caps for the first planar cell have designed and fabricated. Cells have been assembled and tested, including a three cell stack. A five cell stack has been assembled.
Task 3.0: Preparation of the anode, the cathode, and cell fabrication. Both tubular and planar cells have been assembled.
Task 4.0: Electrochemical testing of cells. Both tubular and planar cells have been subjected to charge-discharge cycles.

Results of work done during the fifth quarter are described in this progress report.

SUMMARY OF SIGNIFICANT ACCOMPLISHMENTS

1) BASE has been fabricated by a vapor phase process.
2) Discs and tubes of BASE have been fabricated.
3) $ZnCl_2$ has been identified as cathode for Na/BASE/ZnCl2 battery. The OCV is over 2 V. The battery has operated up to 425^{o}C.
4) Na/BASE/ZnCl2 cells have been subjected to several charge-discharge and freeze-thaw cycles.
5) Planar cells have been fabricated and successfully tested.
6) Other possible cathodes have been identified.
7) BASE with porous surface layers for polarization reduction have been fabricated.
8) A two-cell stack has been assembled and tested.
9) A five cell stack was assembled.

ACTUAL OR ANTICIPATED PROBLEMS

None.

PRODUCT DESCRIPTION OR TECHNOLOGY TRANSFER

None.

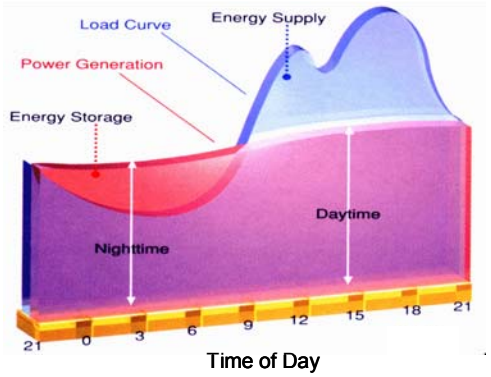

Figure 1: Power demand as a function of time of day. Also shown is the role of an energy storage system on peak shaving.

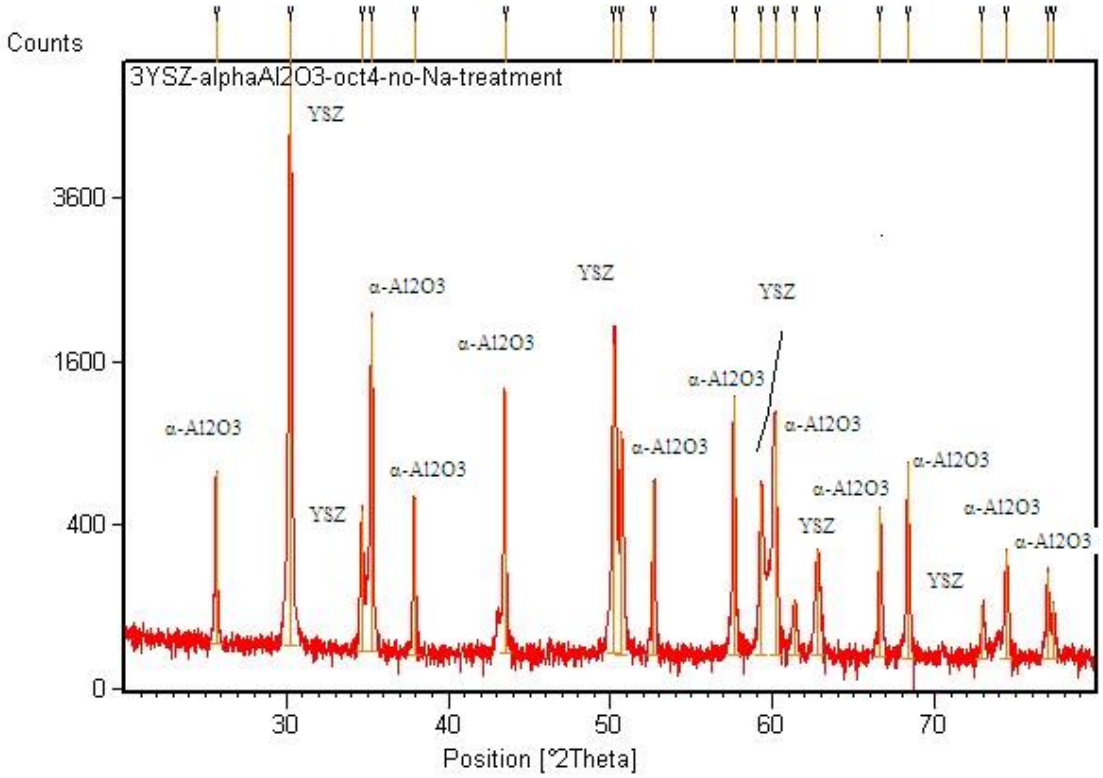

Figure 2: An X-Ray Diffraction pattern of CR-30/ TZ-3Y sample. Note the presence of XRD peaks of both alumina and YSZ.

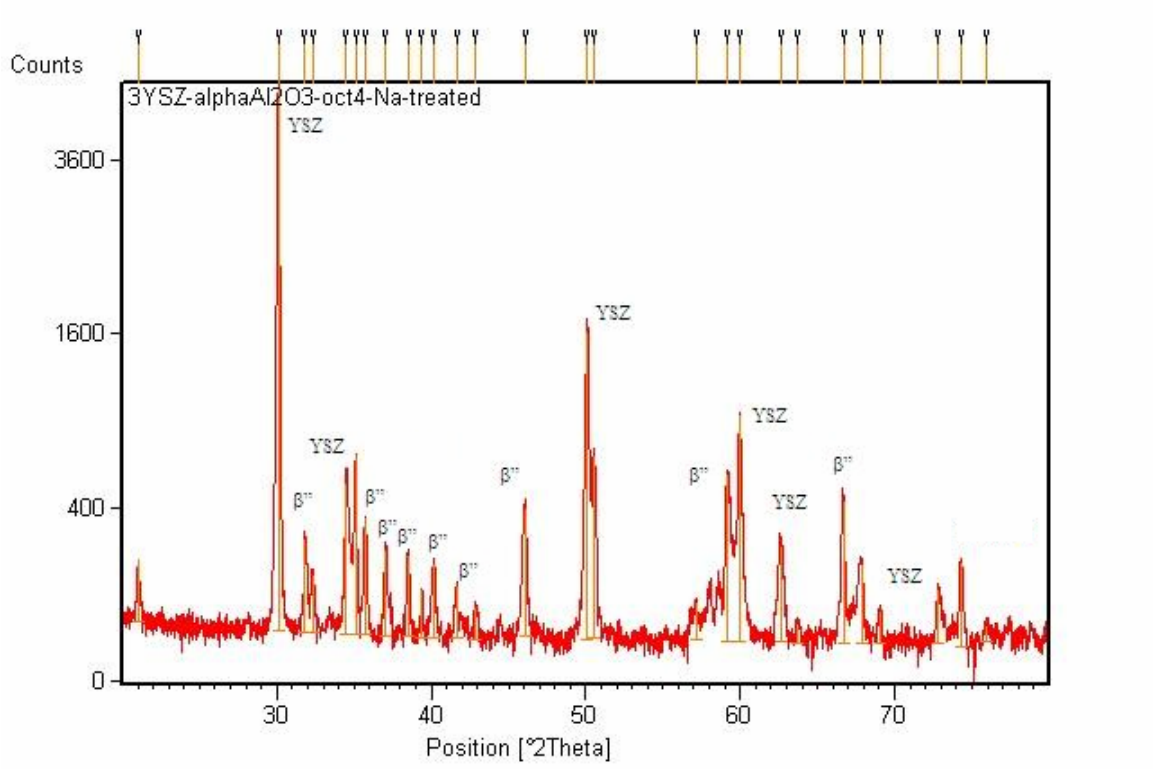

Figure 3: An X-Ray Diffraction Pattern of BASE sample after conversion. Note the presence of XRD peaks of BASE (β"-alumina) and YSZ.

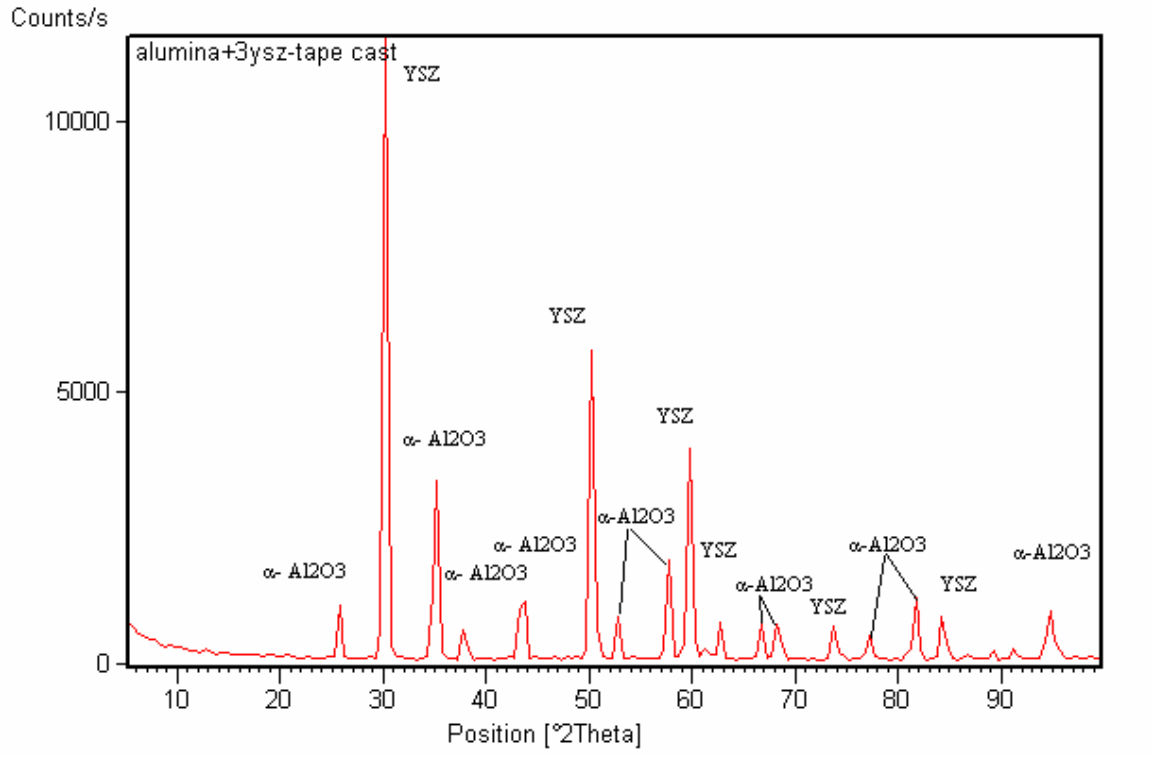

Figure 4: X-Ray Diffraction pattern of as-sintered tape cast sample.

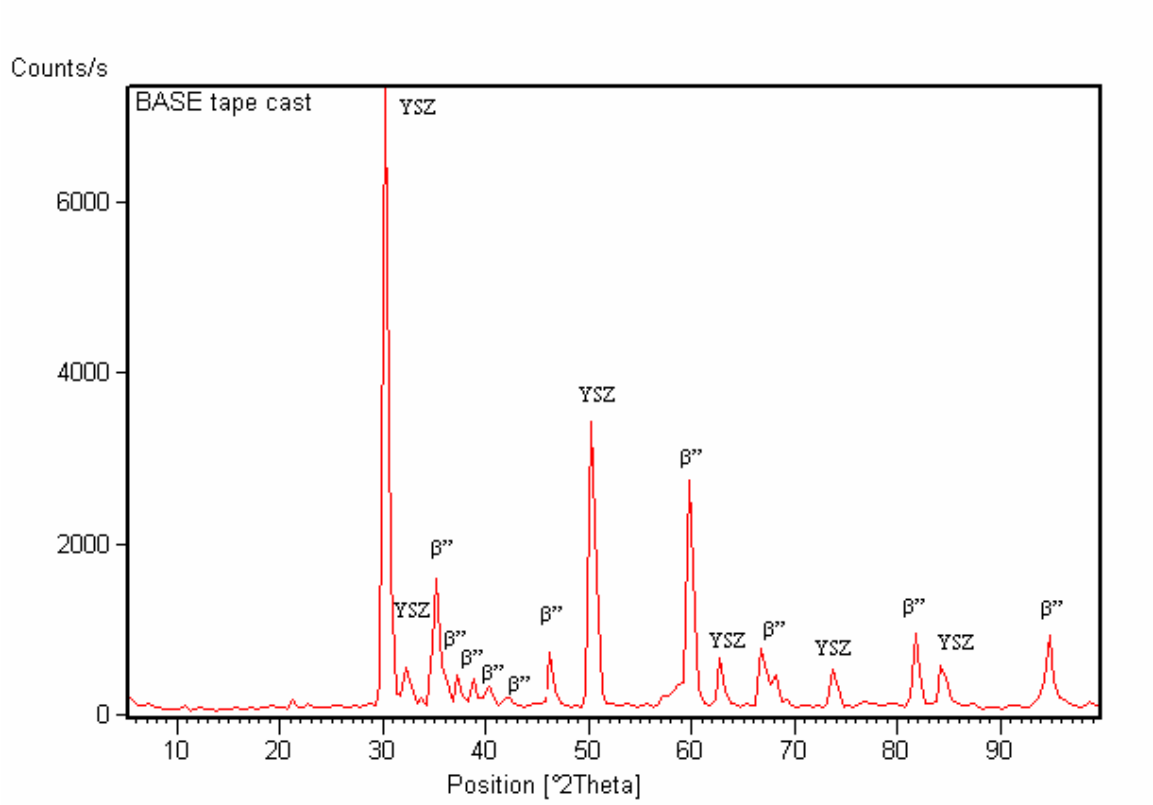

Figure 5: X-Ray Diffraction Pattern of tape cast sample after conversion to BASE.

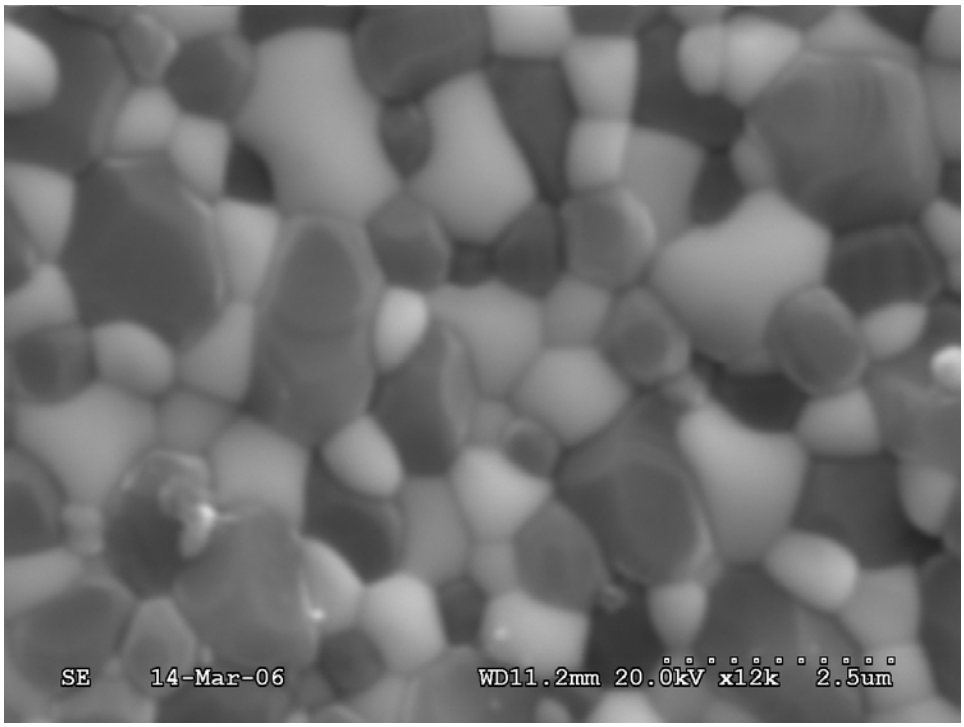

Figure 6: Microstructure of as – sintered tape cast sample

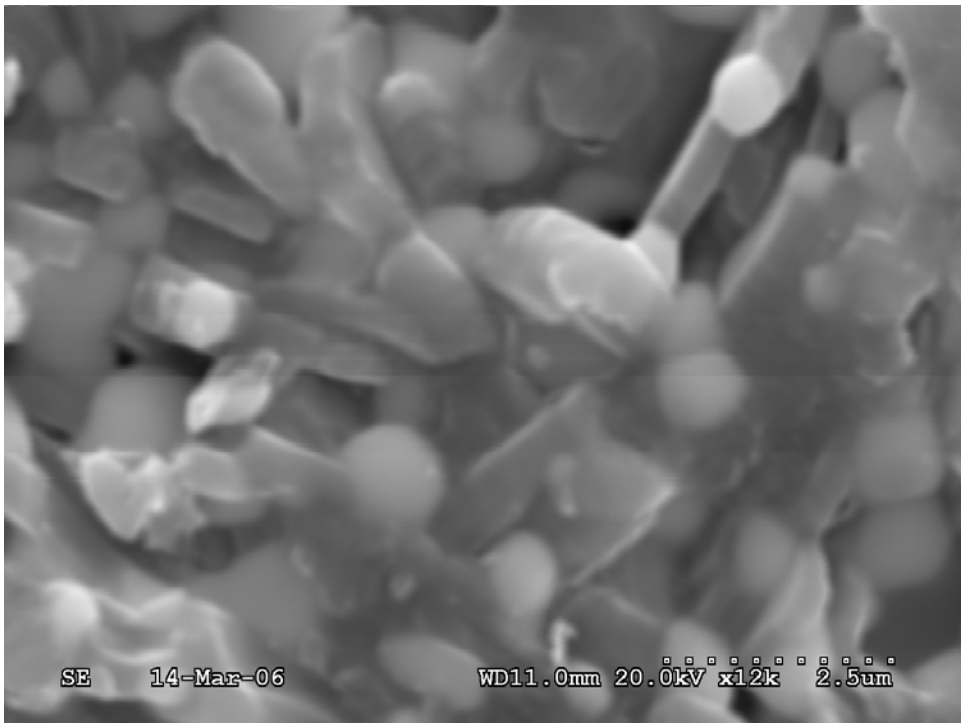

Figure 7: An SEM image of the sample after conversion to BASE. Note the tabular BASE grains.

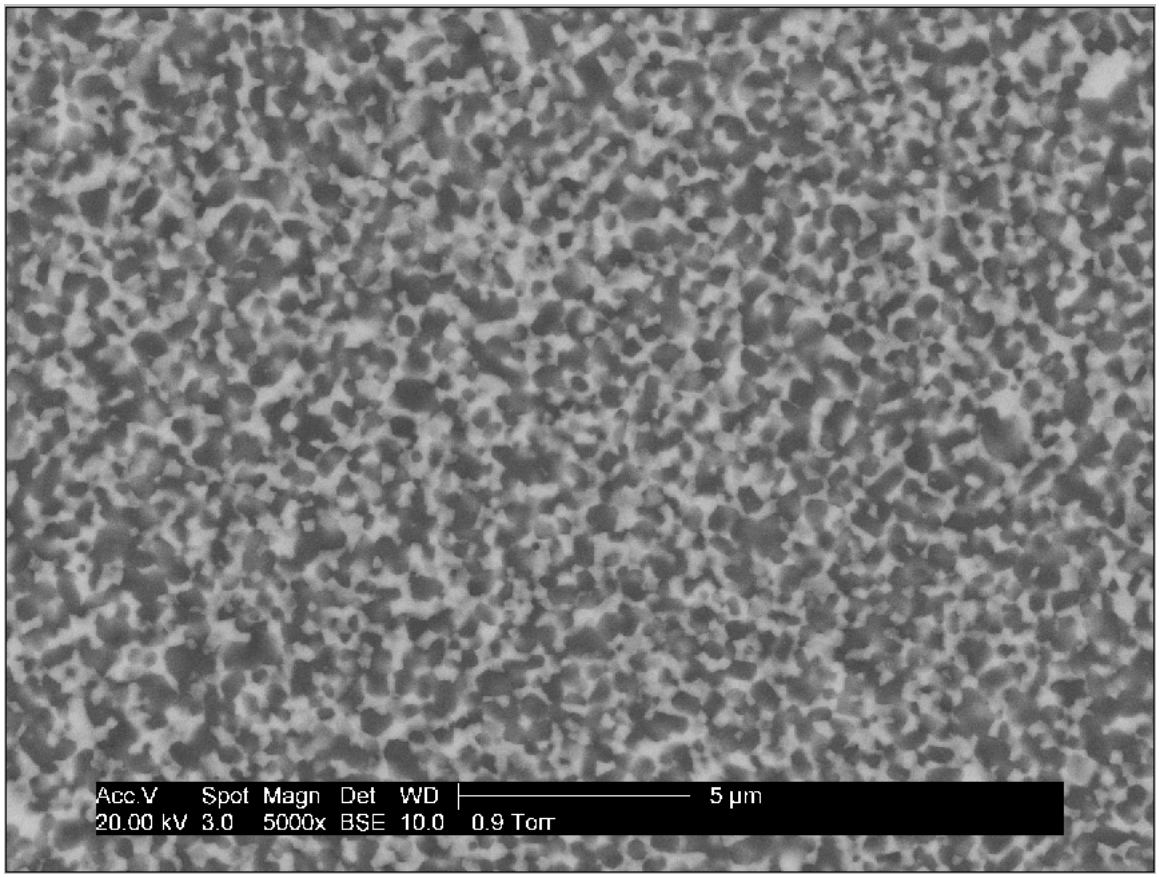

Figure 8: Microstructure of α-alumina + 3YSZ sample sintered at 1500^{o}C for 1 hour. The grey areas are alumina and white areas are YSZ. The average grain size is 0.53 µm.

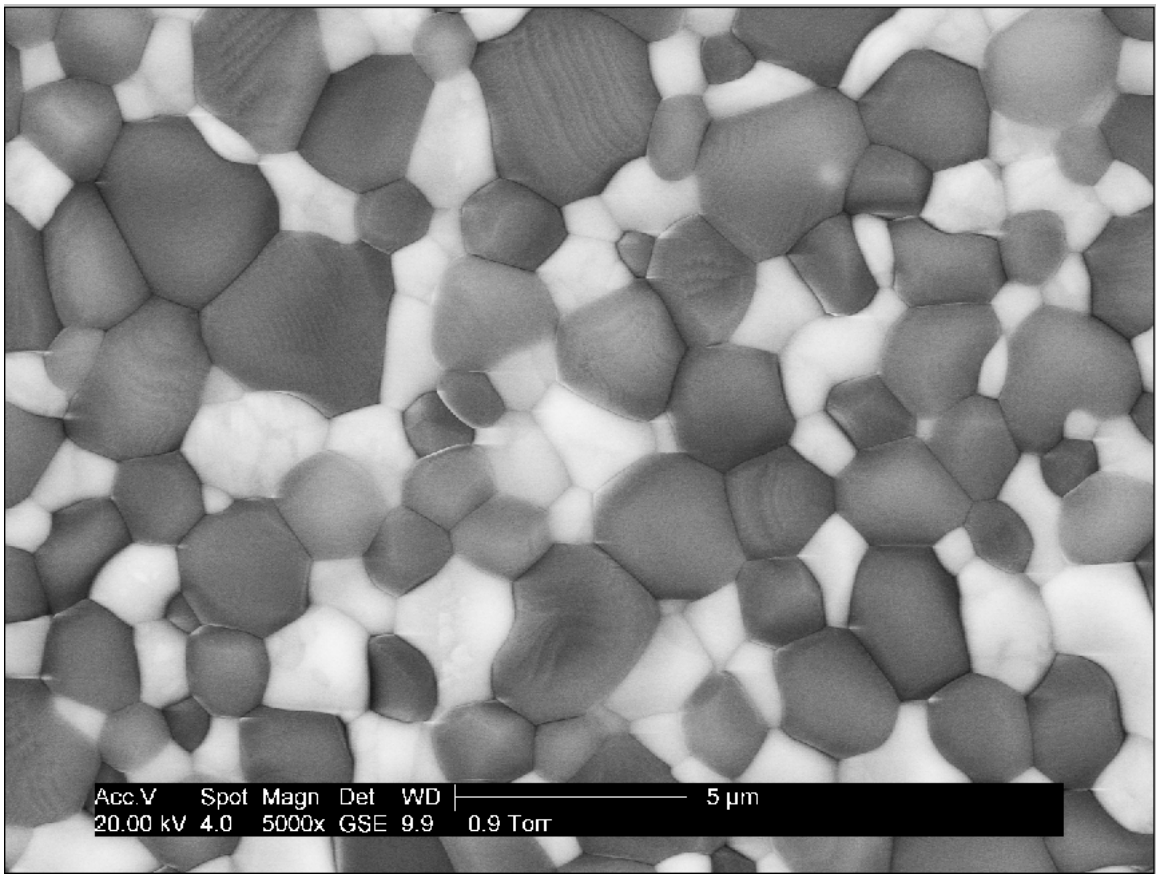

Figure 9: Microstructure of α-alumina + 3YSZ sample sintered at 1800^{o}C for 1 hour. The grey areas are alumina and white areas are YSZ. The average grain size is 2.70 µm.

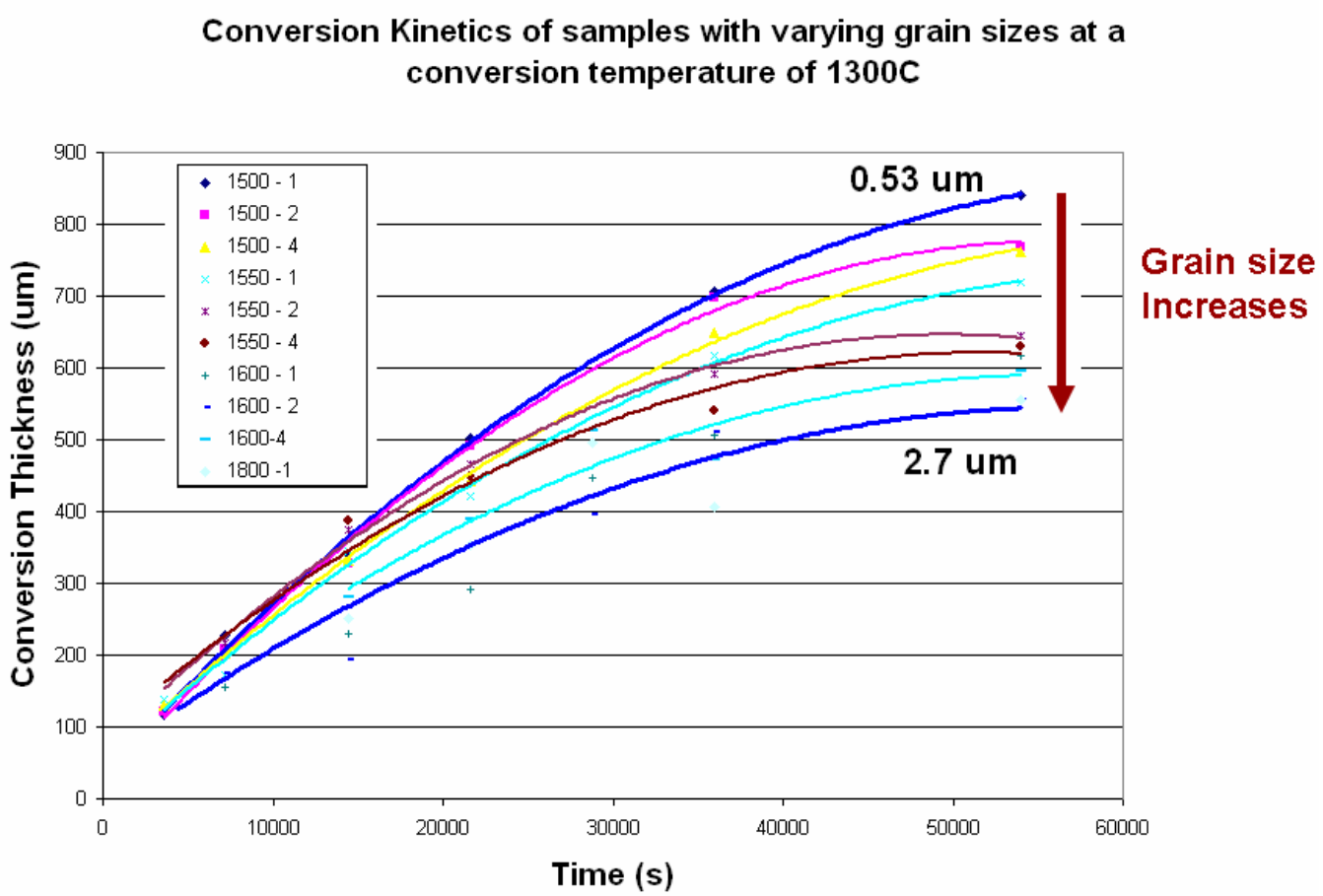

Figure 10: Conversion Thickness as a function of hold time for the samples with varying grain sizes, Conversion Temperature – 1300^{o}C.

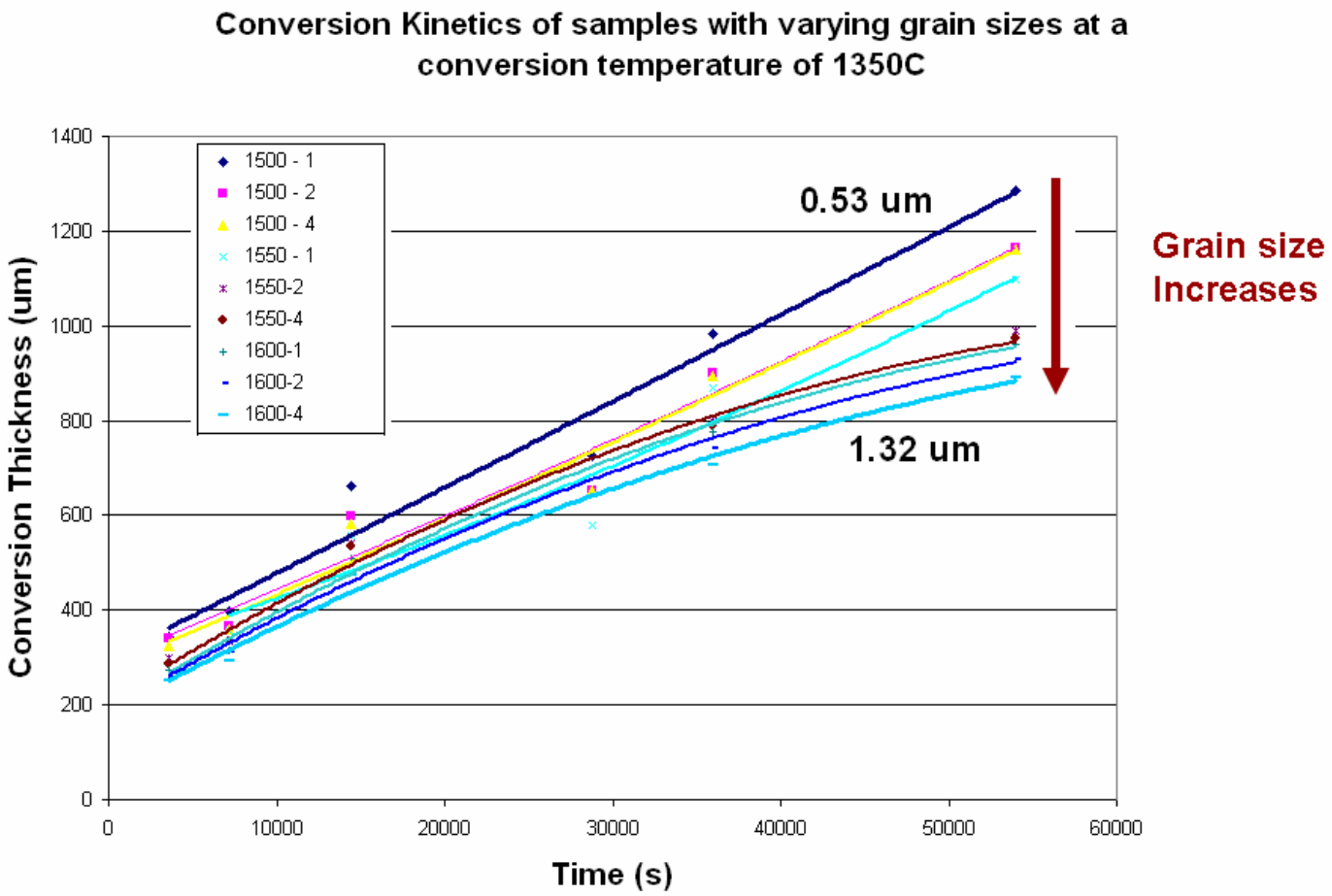

Figure 11: Conversion Thickness as a function of hold time for the samples with varying grain sizes, Conversion Temperature – 1350^{o}C.

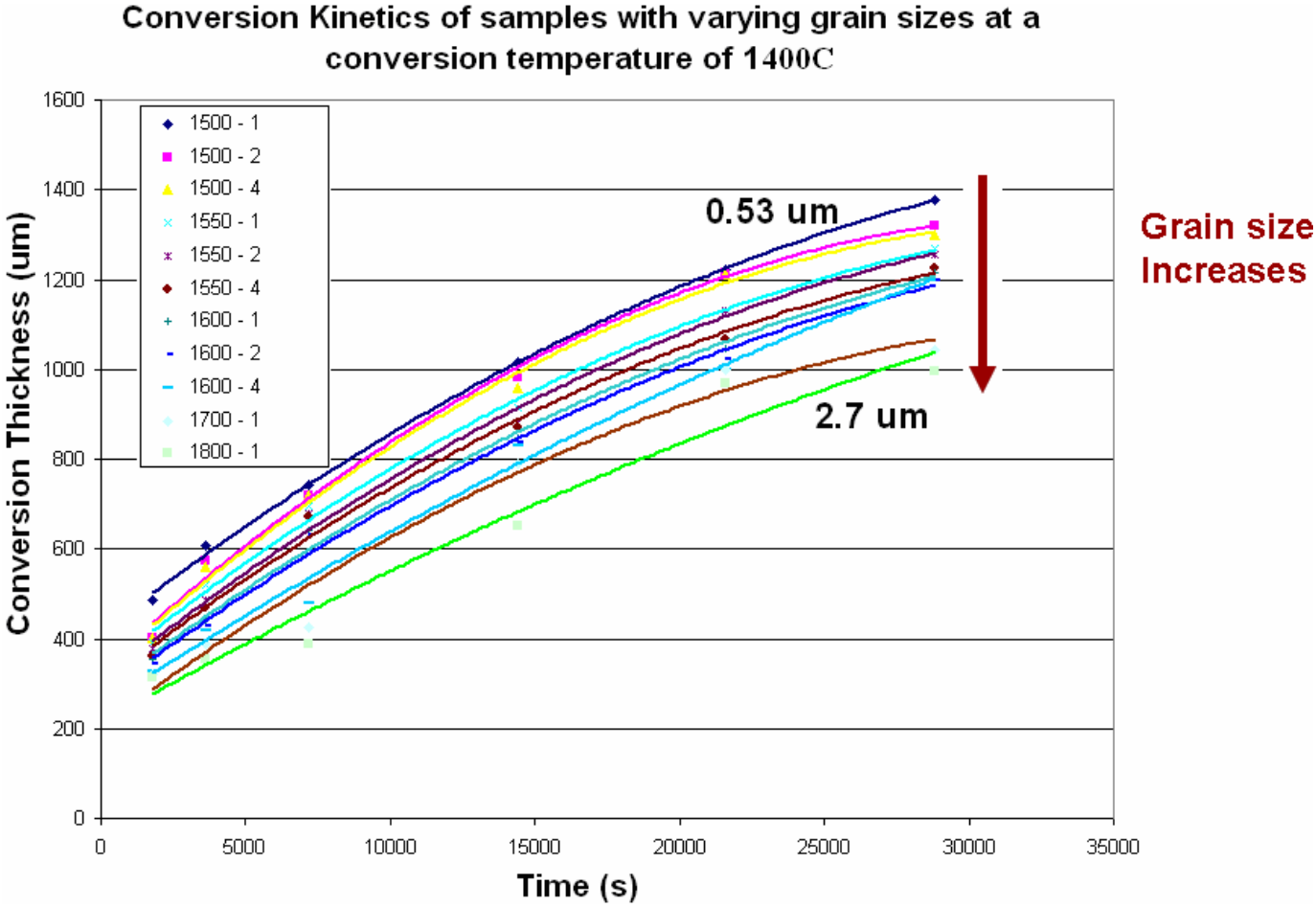

Figure 12: Conversion Thickness as a function of hold time for the samples with varying grain sizes, Conversion Temperature – 1400°C.

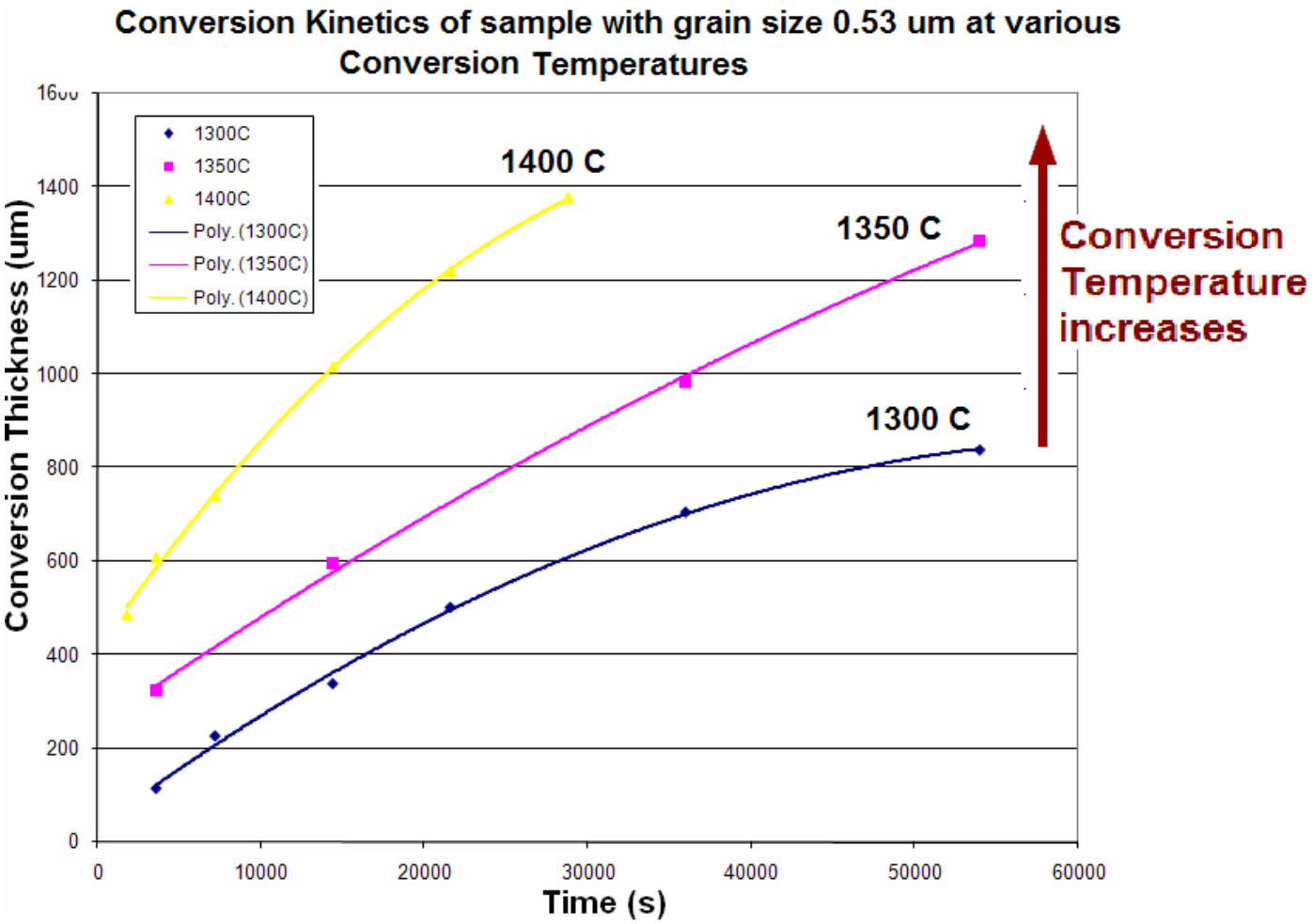

Figure 13: Conversion Kinetics as a function of hold time for the sample with a grain size of 0.53 μm at various conversion temperatures.

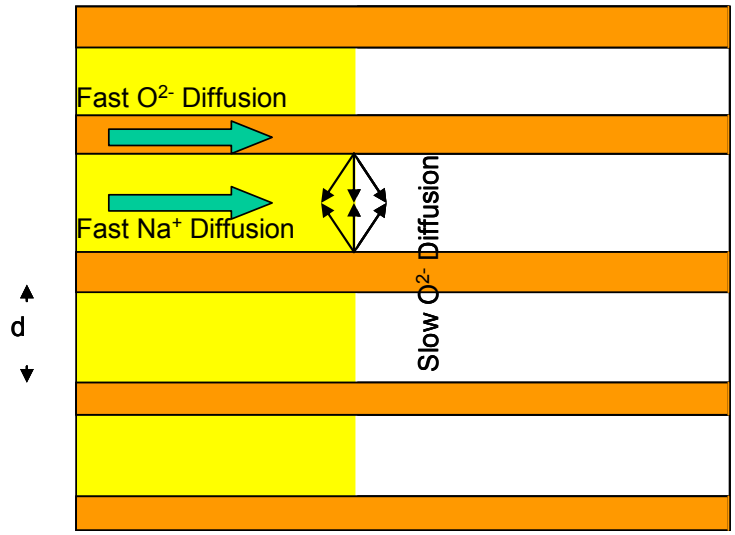

Fixed Diffusion Distance
Linear Kinetics

$$x \approx Kt \qquad K \sim f\left(\frac{1}{d}\right)$$

Figure 14: The mechanism of conversion of a-alumina into BASE.

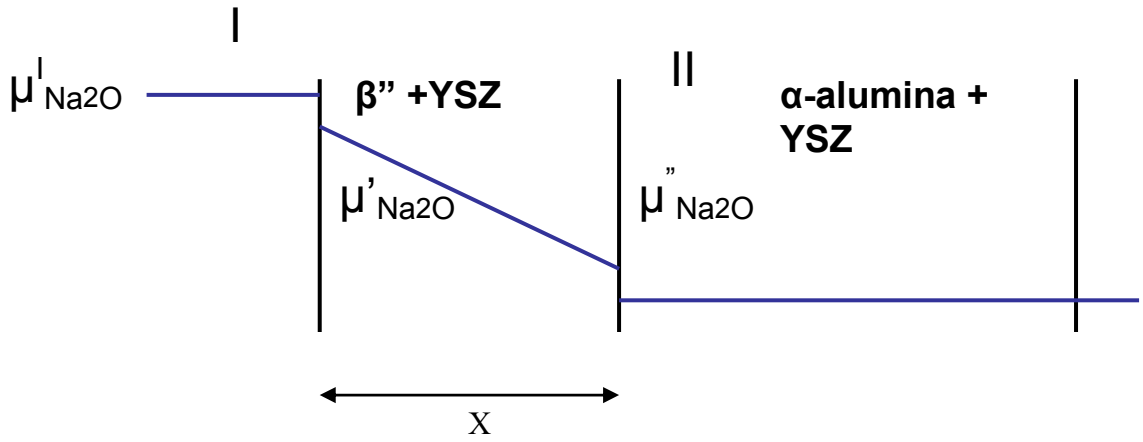

Figure 15: A schematic showing the kinetics of conversion. The process involves two interfacial steps and one diffusive (coupled) step.

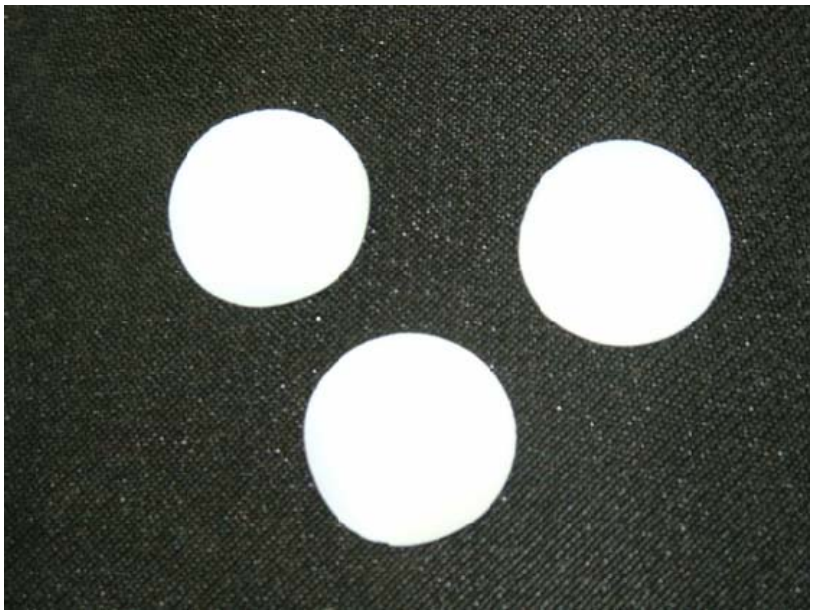

Figure 16: Tape cast samples of BASE discs of thickness 0.8mm and diameter 2.1 inches.

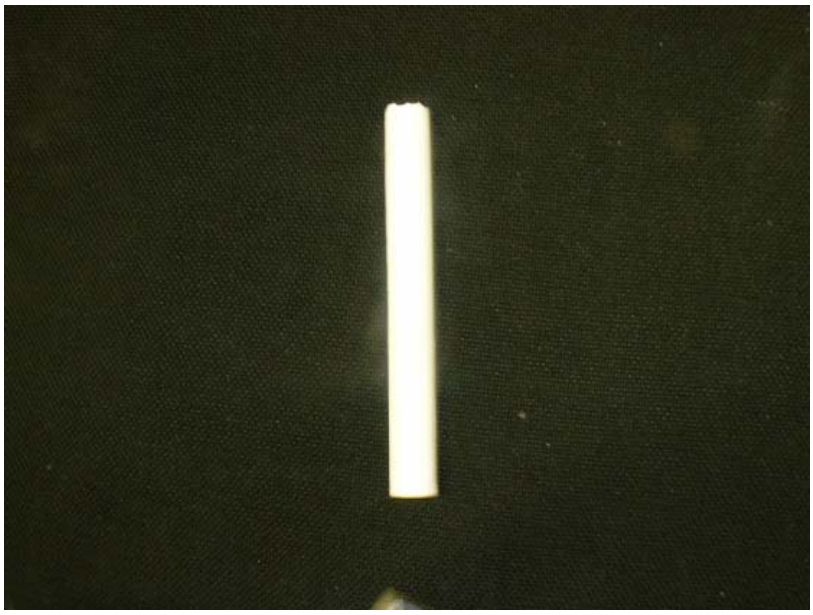

Figure 17: Slip cast sample of BASE tube with wall thickness of 1mm.

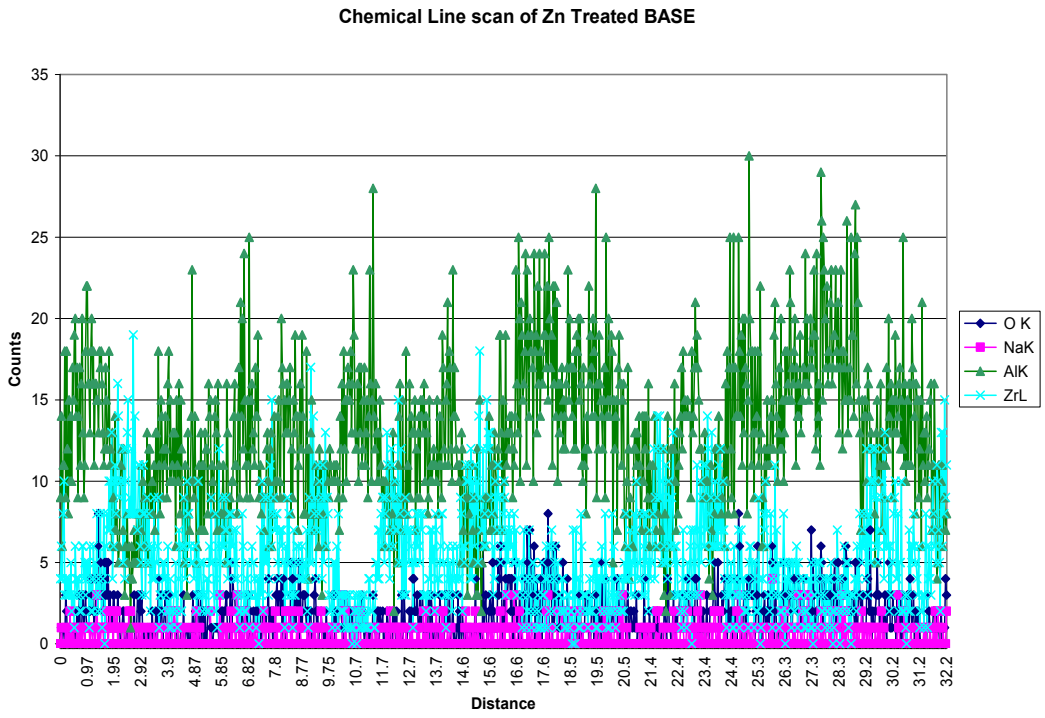

Figure 18: Chemical line scan of BASE after treating with Zinc Chloride for 22 h at 430°C. No Zn was detected in the BASE indicating that no ion exchange occurred.

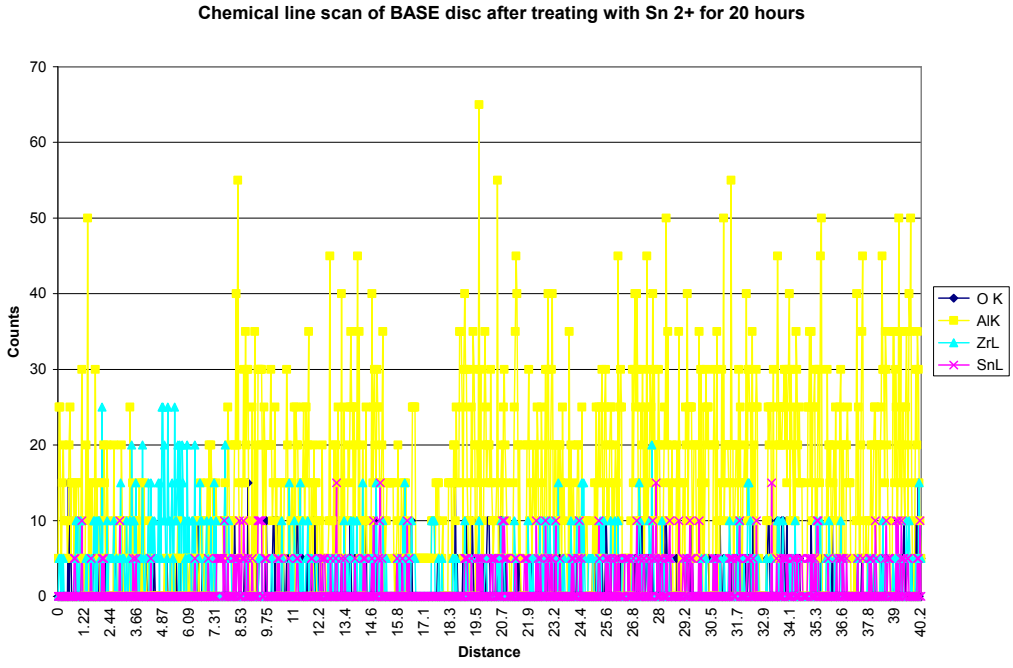

Figure 19: Chemical line scan of BASE sample after treating with $SnCl_2$ for 20 hours. Sodium is completely replaced by Sn.

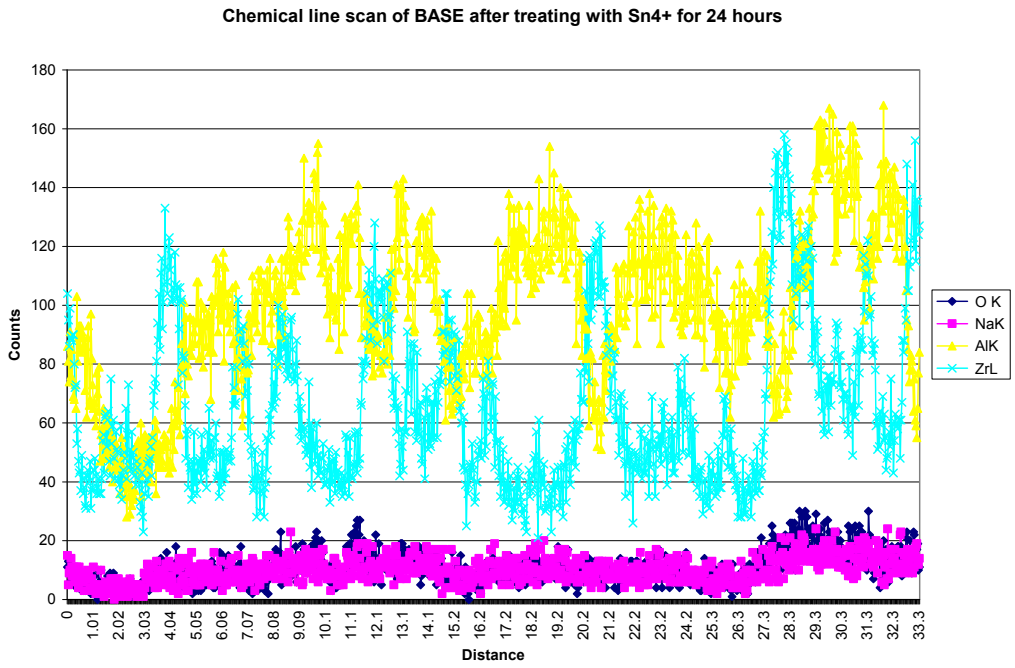

Figure 20: Chemical line scan of BASE samples after treating with SnI_4 for 24 hours. No Sn is found in the sample, indicating no ion exchange occurred.

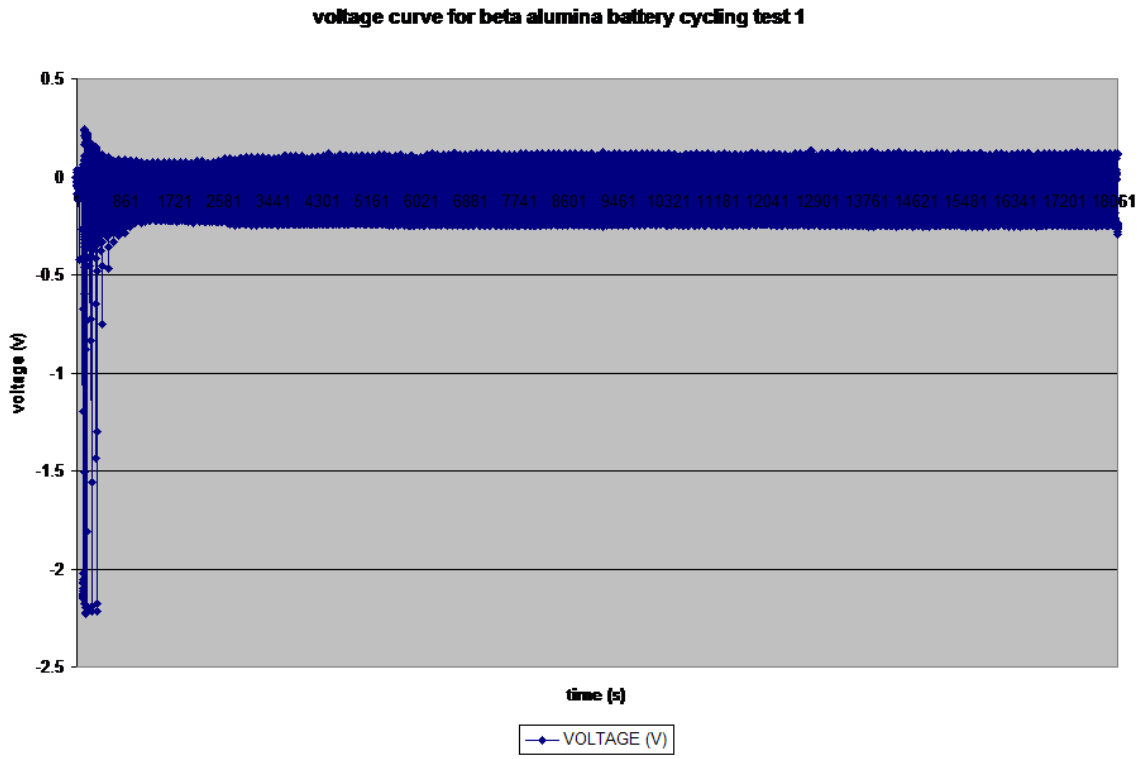

Figure 21: Voltage response of the conductivity measurement of the BASE tube using eutectic composition on both sides. Note that there is no rise in voltage (indicating there is no rise in resistance). The test was run for about 5 hours.

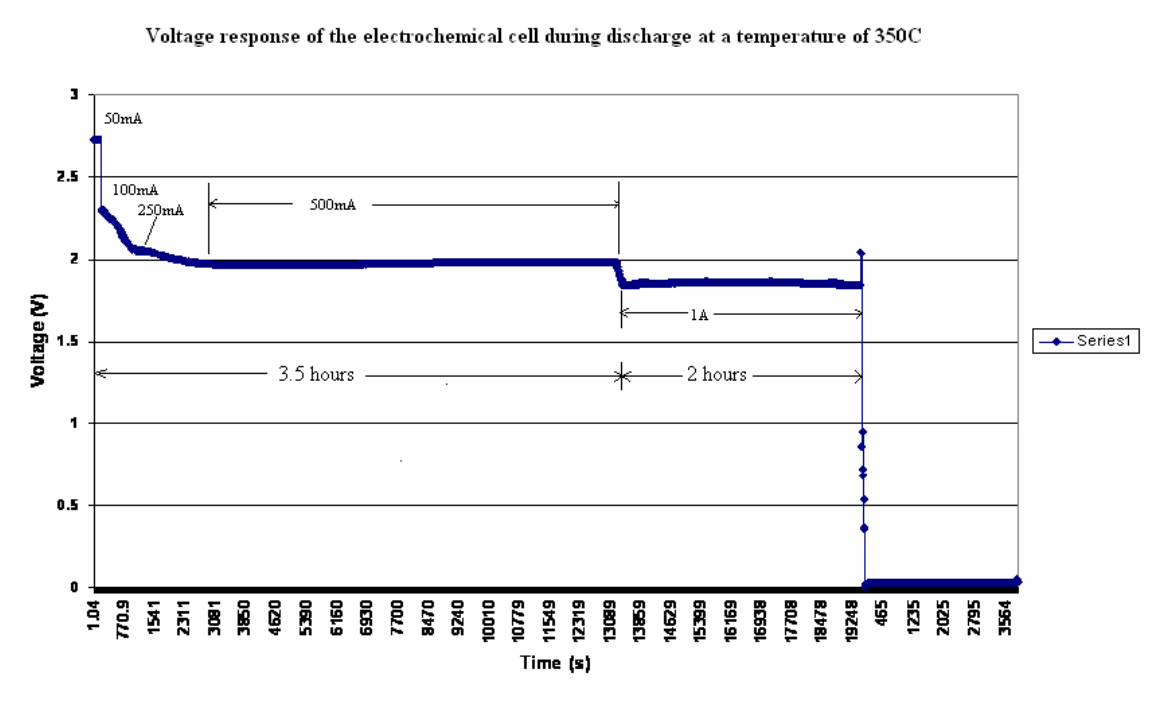

Figure 22: Voltage response during the discharge of the electrochemical cell assembled in the fully charged state.

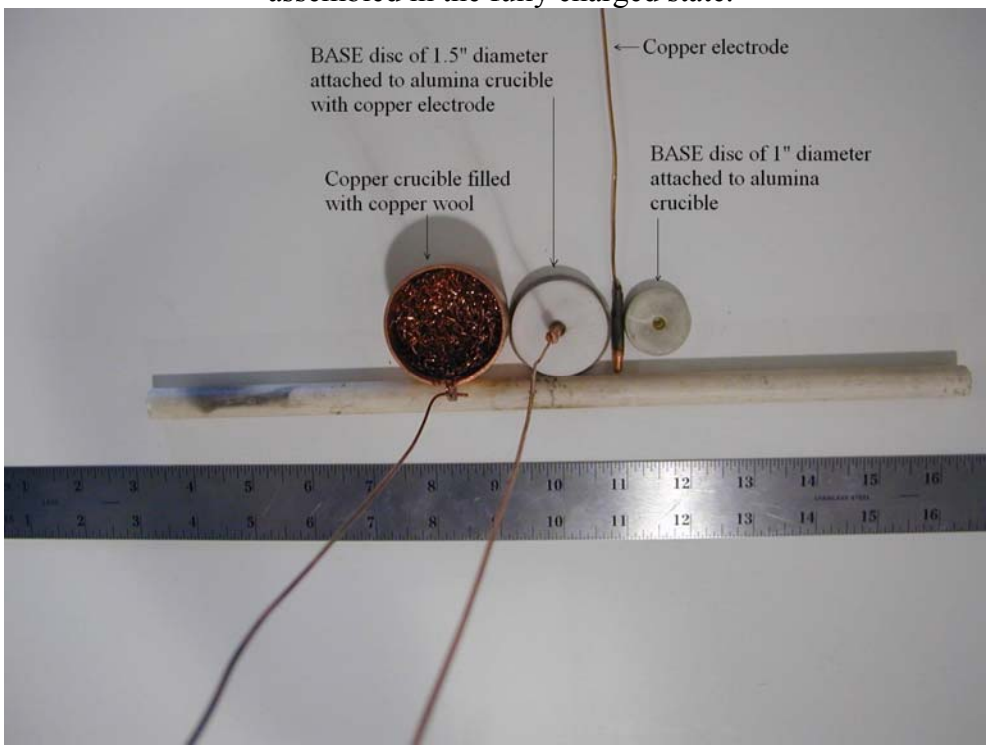

Figure 23: Cathode side and anode – electrolyte set up of planar cell.

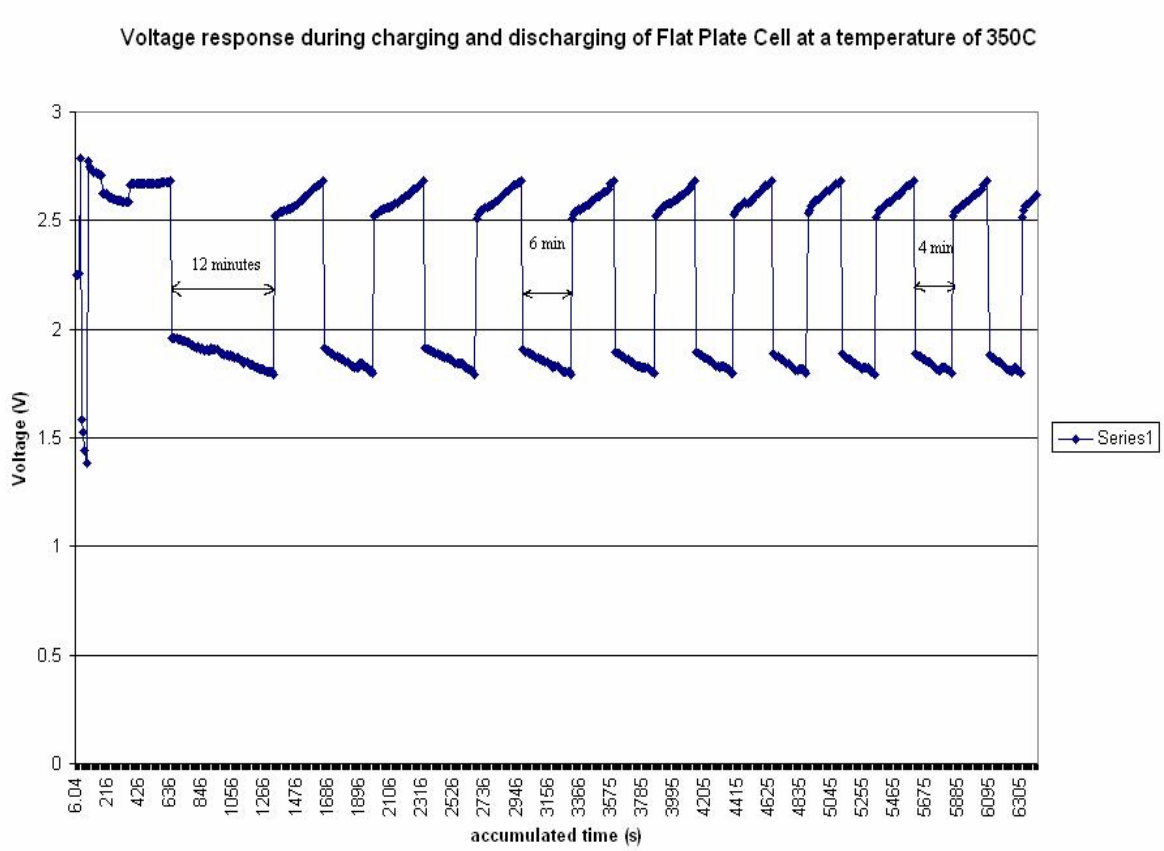

Figure 24(a): Voltage response of the charging and discharging of planar cell assembled in the partially charged state.

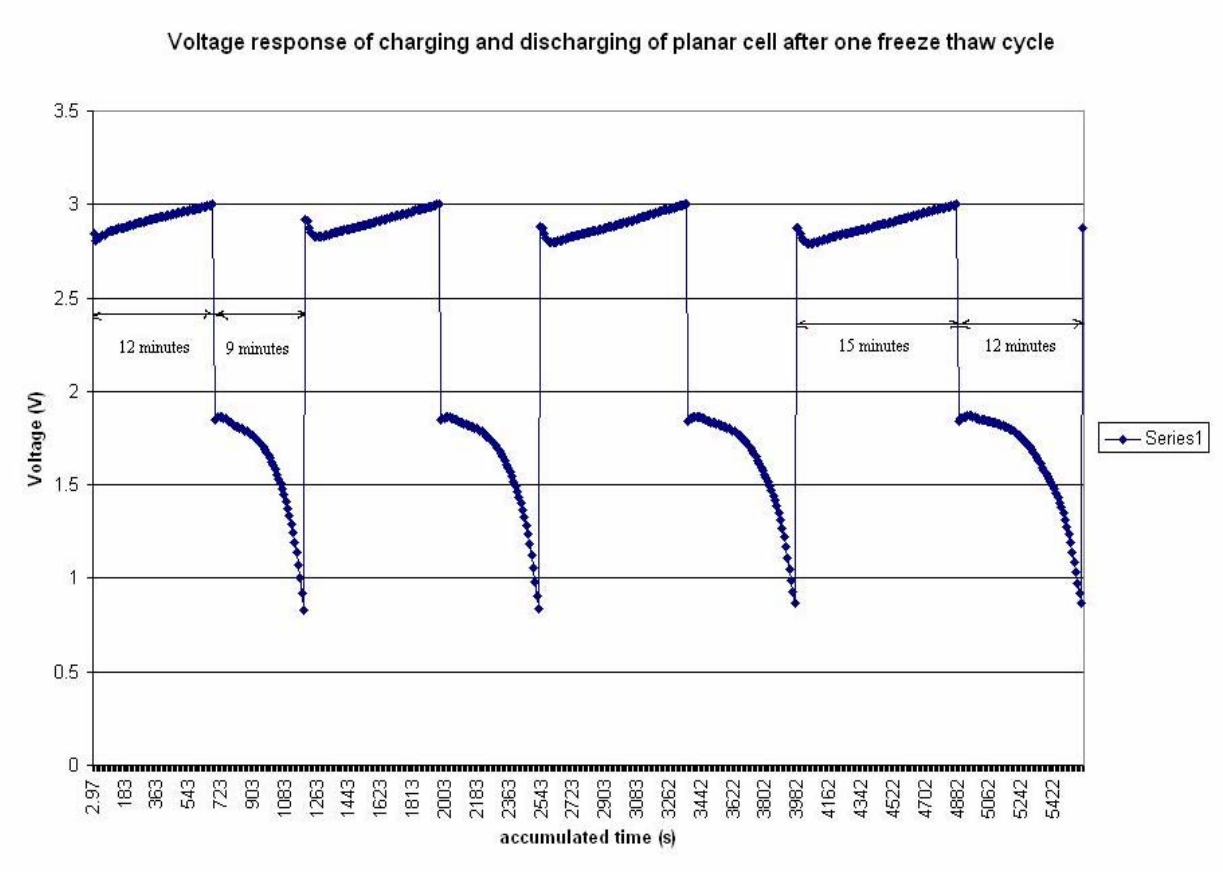

Figure 24(b): Voltage response of the charging and discharging of the planar cell after one freeze thaw cycle.

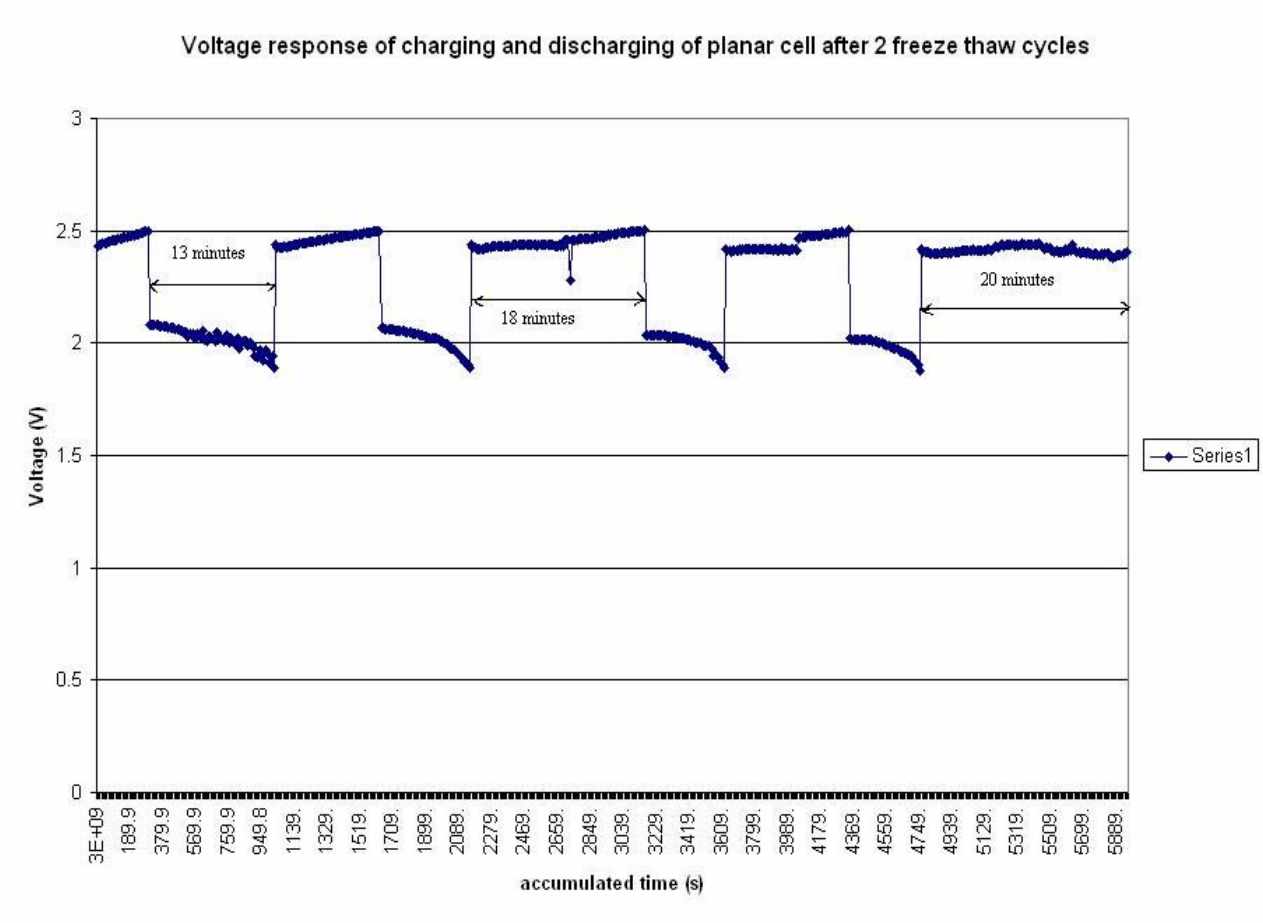

Figure 24(c): Voltage response of the charging and discharging of the planar cell after two freeze thaw cycles.

Figure 25: Components of a planar cell.

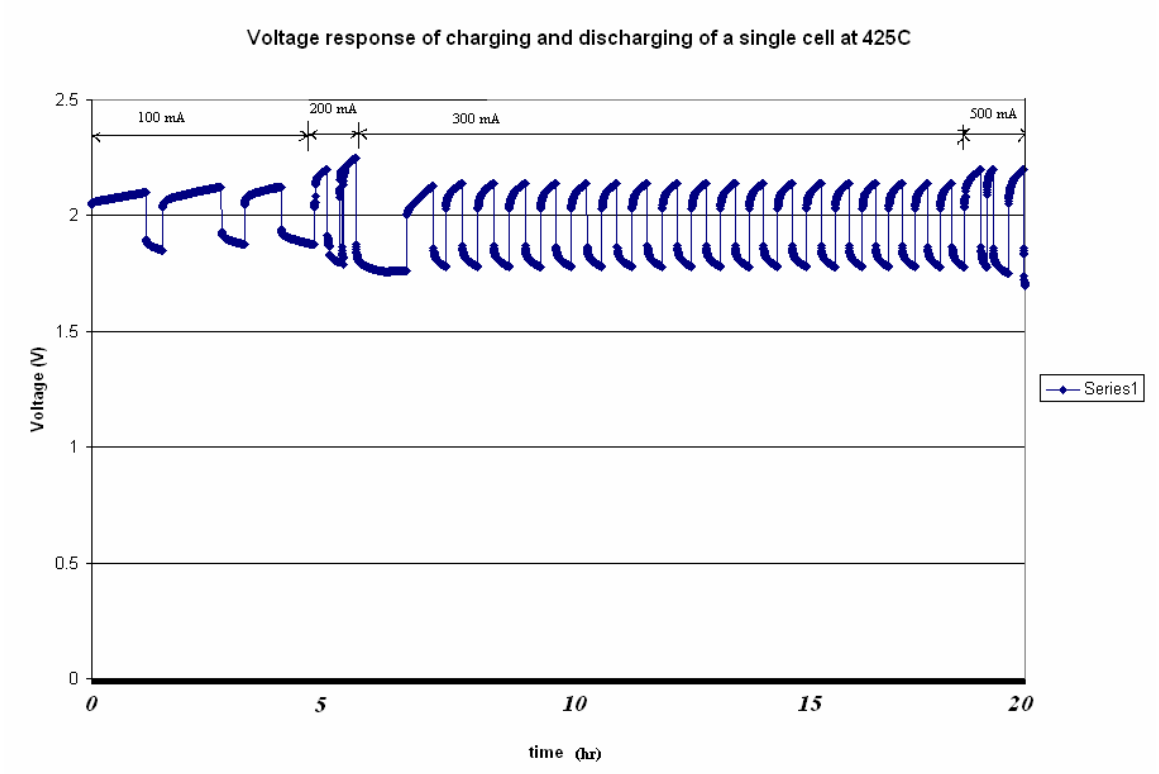

Figure 26: Voltage response during charging and discharging of the planar cell at a temperature of 425°C, above the melting point of zinc. The cell was operated for 50 hours. The figure shows only a part of it (20 hours).

Figure 27: The planar three cell stack assembly used for testing.

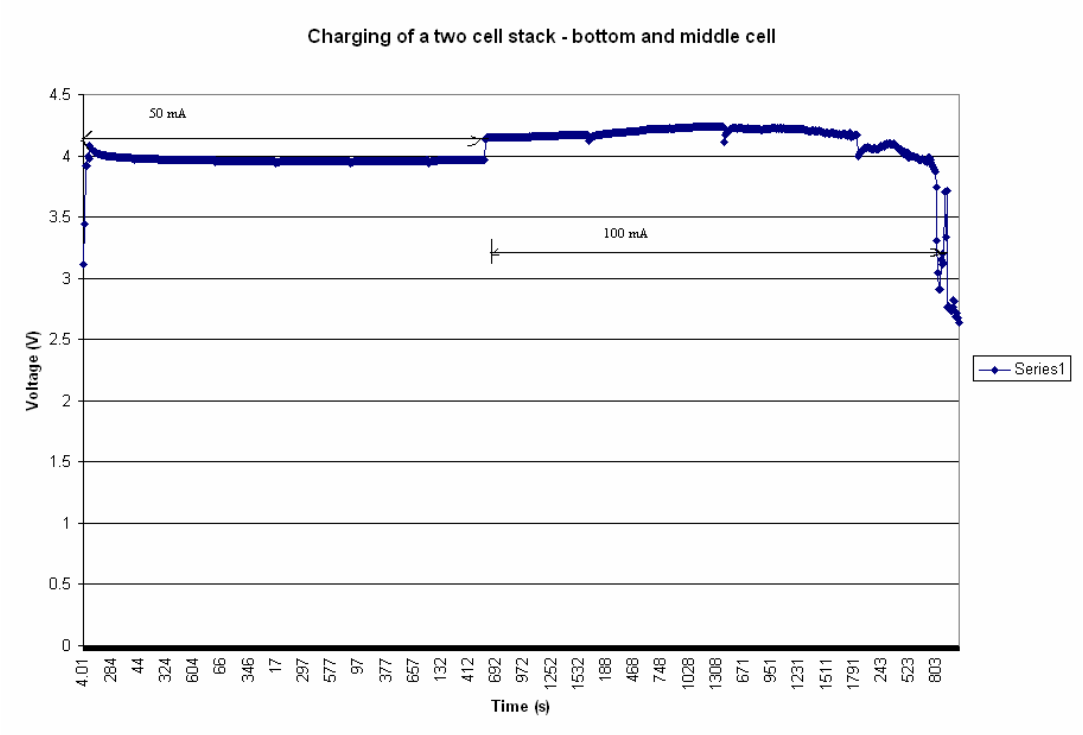

Figure 28: Voltage response of the charging of two cell stack at an operating temperature of 400^{o}C. Voltage is reduced at the end as one of the cell was shorted at that point.

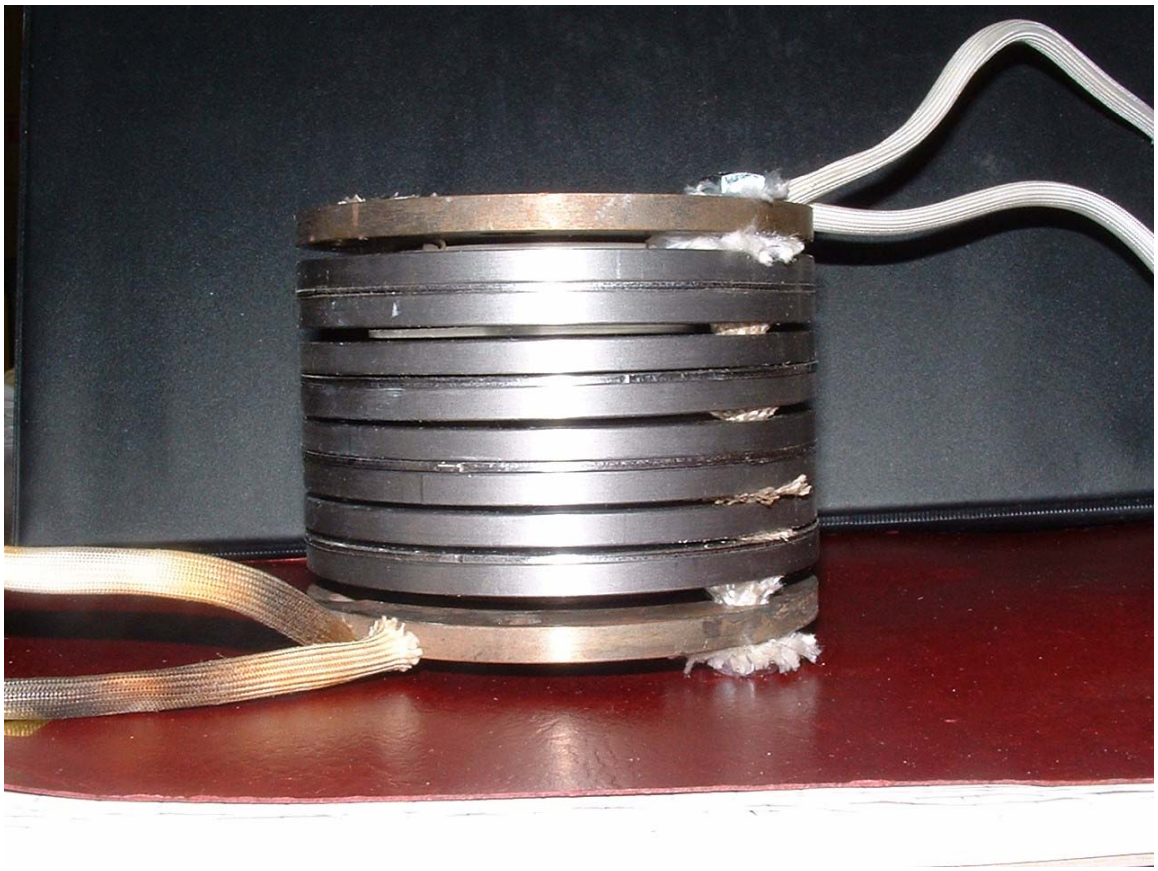

Figure 29: A five cell stack.

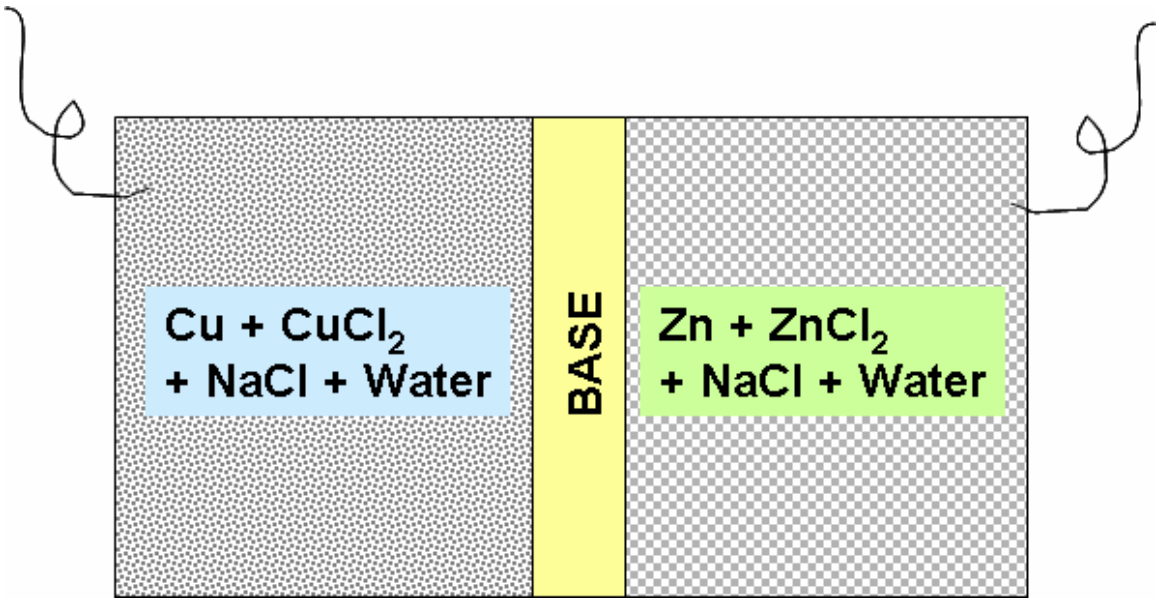

Figure 30: A schematic of an aqueous cell made using BASE.

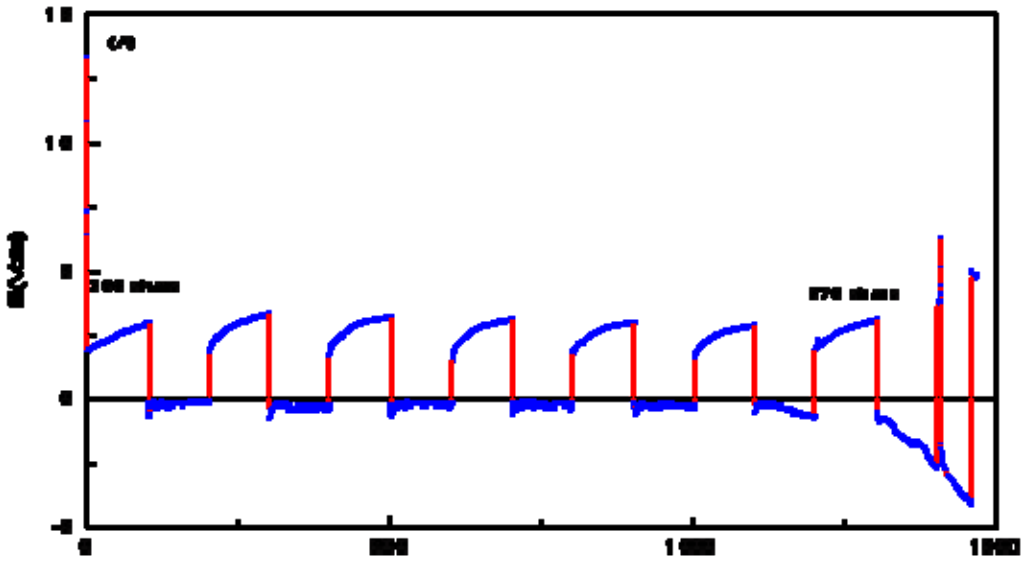

Figure 31: An electrochemical cell with aqueous liquids at the two electrodes. The BASE disc was without porous electrodes. The cell resistance was initially ~308 Ω and increased to ~570 Ω after a period of time.

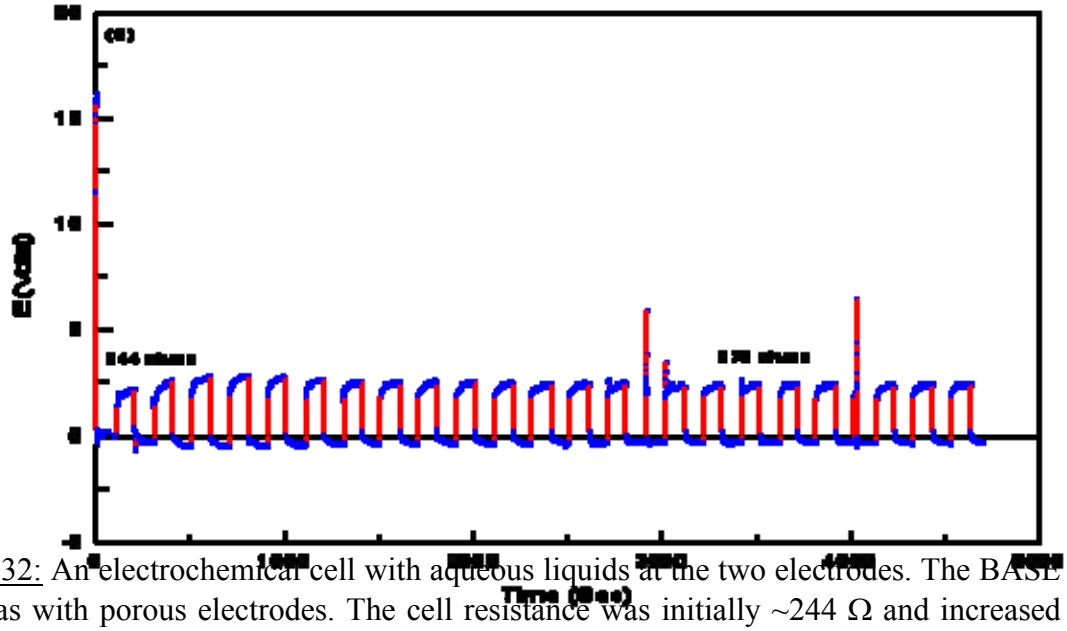

Figure 32: An electrochemical cell with aqueous liquids at the two electrodes. The BASE disc was with porous electrodes. The cell resistance was initially ~244 Ω and increased slightly to ~270 Ω after a period of time. Note that the cell resistance was considerably lower than the cell without porous layers.

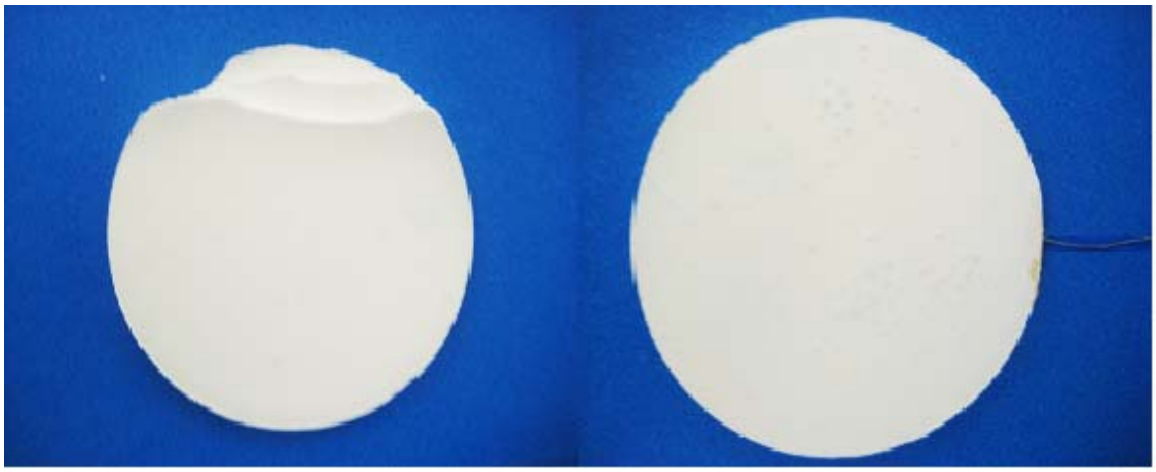

Figure 33: a) Delaminated BASE electrolyte with Platinum electrodes embedded (left). b) BASE electrolyte with embedded Platinum electrodes and platinum wire attached to the electrodes (right).

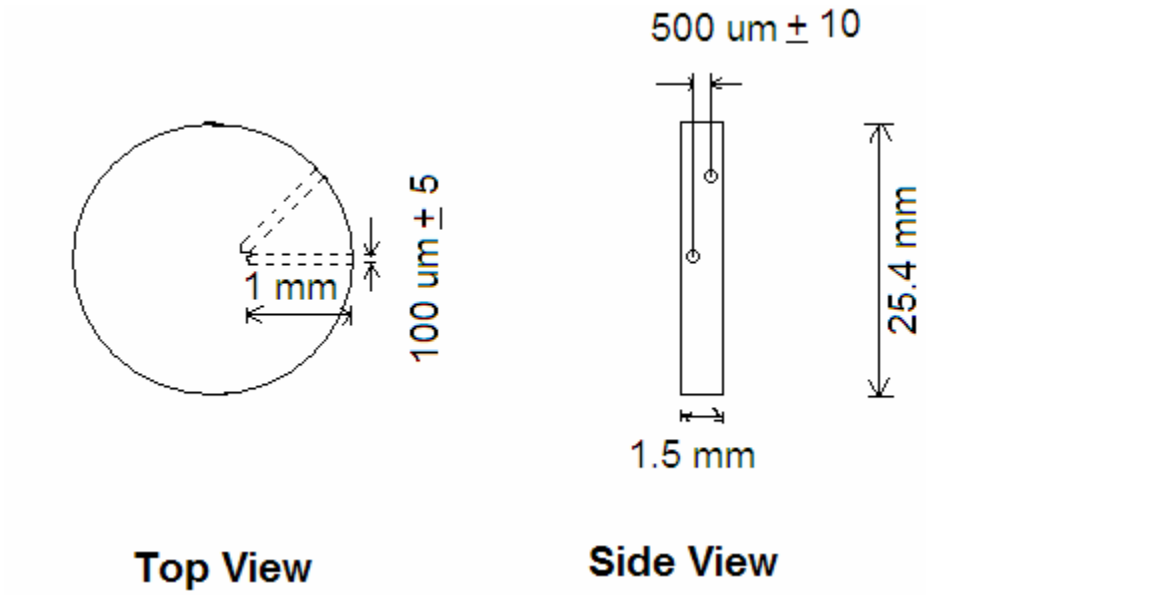

Figure 34: Schematic of the electrolyte disc with micro drilled holes of diameter 100 µm.

LIST OF ACRONYMS AND ABBREVIATIONS

BASE	Beta" alumina solid electrolyte
kWh	Kilo watt hours
MWh	Mega watt hours
OCV	Open Circuit Voltage
PEM	Proton exchange membrane
SEM	Scanning electron microscope
SOFC	Solid oxide fuel cell
XRD	X-ray diffraction
YSZ	Yttria-stabilized zirconia
ZEBRA	Zero Emission Batteries